Russian Journal of Earth Sciences Online ISSN: 1681-1208

Special Issue: "Kamchatka Earthquake M 8.8 on July 29, 2025"

Long-Term Earthquake Prediction by S. A. Fedotov for the Kuril–Kamchatka Arc and the Kamchatka Megathrust Earthquake of July 29, 2025. Review

A. D. Gvishiani[1,2], **A. O. Gliko**[2], **B. A. Dzeboev**[1,2,*], **B. V. Dzeranov**[1], **and E. O. Kedrov**[1]

[1]Geophysical Center of the Russian Academy of Sciences, Moscow, Russian Federation
[2]Schmidt Institute of Physics of the Earth of the Russian Academy of Sciences, Moscow, Russian Federation
* **Correspondence to:** Boris Dzeboev, b.dzeboev@gcras.ru

Dedicated to the outstanding Soviet and Russian seismologist Sergey A. Fedotov (1931–2019)

Abstract: On July 29, 2025, an earthquake with a moment magnitude of $M_W = 8.8$ occurred in the Kuril–Kamchatka Trench to the east of Petropavlovsk-Kamchatsky. This earthquake ranks among the ten strongest instrumentally recorded seismic events in the world. For the first time, a megathrust earthquake of such magnitude (greater than 8.5) caused no human casualties or mass destruction. This was largely due to the advanced implementation of preventive measures on the territory of Kamchatka Krai. These measures included the targeted strengthening of the seismic resistance of buildings and structures, as well as the enhancement of alert and population evacuation algorithms. The scientific basis for planning these seismic safety measures was provided by the long-term earthquake prediction carried out Dr. Sergey A. Fedotov, full member of the Russian Academy of Sciences. This paper is devoted to a contemporary reassessment of the results of long-term earthquake prediction for the Kuril–Kamchatka island arc by S. A. Fedotov in the context of the 2025 Kamchatka megathrust earthquake. The paper details the development and evolution of the method, which is grounded in the concepts of seismic gaps and the seismic cycle. The cycles of seismic activity and seismic energy release in the source area of the strongest earthquake, as constructed by S. A. Fedotov, together with the foreshock–aftershock scenario, are presented. The paper describes the long-term earthquake predictions for five-year periods and provides an overall assessment of their reliability. It is shown that, since 1965, the sources of all earthquakes with $M \geq 7.75$ have occurred within the seismic gaps that S. A. Fedotov had identified as the most probable areas of the future strongest earthquakes. The source of the 2025 megathrust earthquake originated in a region that, as early as the beginning of the 1980s, had been identified as one of the segments of the Kuril–Kamchatka Arc where the next strongest earthquakes were expected. According to a refined prediction made in 2019, the probability of a megathrust earthquake occurring in that area within the following five-year period was estimated at 50.4%. Thus, the long-term earthquake prediction method by S. A. Fedotov has been successfully verified by a planetary-scale event. The 2025 Kamchatka megathrust earthquake has convincingly confirmed its fundamental tenets, indicating the high predictive efficiency of the method.

Review

Received: February 2, 2026
Accepted: May 25, 2026
Published: July 1, 2026

Keywords: S. A. Fedotov, long-term earthquake prediction, seismic cycle, seismic gaps, Kuril–Kamchatka Arc, Pacific Ring of Fire, Kamchatka megathrust earthquake, seismic hazard

Citation: Gvishiani A. D., Gliko A. O., Dzeboev B. A., Dzeranov B. V., and Kedrov E. O. (2026), Long-Term Earthquake Prediction by S. A. Fedotov for the Kuril–Kamchatka Arc and the Kamchatka Megathrust Earthquake of July 29, 2025. Review, *Russian Journal of Earth Sciences*, 26, ES2001, EDN: JCTKJG, https://doi.org/10.2205/2026es001111

1. Introduction

The Pacific Ring of Fire is the vastest and the most tectonically active region in the world [*Bilek and Lay*, 2018]. With a total length of over 40,000 km, it arcs around the Pacific Ocean. The Ring extends from the western coasts of South and North America to the Aleutian Islands, and then southward along the Kuril–Kamchatka Island Arc, Japan, and the Philippines, reaching Indonesia and New Zealand. There is a high population density in many coastal areas of the Pacific Ring of Fire. This makes the assessment of hazards from endogenous and exogenous processes a matter of national security for many countries. Significant results in assessing the seismic hazard of the Pacific Ring as a single entity were achieved as early as the late 1970s using pattern recognition methods [*Gvishiani et al.*, 1978, 1980].

Plate tectonics forms the foundation for understanding the factors that shape the seismicity of the Pacific Ring. A crucial factor is the movement of the Pacific Plate at a rate of several centimeters per year, predominantly in a northwestern direction [*DeMets et al.*, 2010]. In the early 1960s, J. Tuzo Wilson proposed the concept of hotspots (mantle plumes) to describe the movement of the Pacific Plate [*Wilson*, 1963]. Using the Hawaiian Islands as an example, he hypothesized that this chain of volcanic islands and seamounts was formed as the plate moved over a mantle plume. Thus, he explained the linear and age progression of the Hawaiian-Emperor seamount chain and quantified the movement of lithospheric plates [*Yuan et al.*, 2007].

The Pacific Ring of Fire is a zone of interaction between the Pacific Plate and the surrounding continental and oceanic plates. The Ring comprises several zones of tectonic activity, the most prominent being subduction zones characterized by numerous volcanoes, earthquakes, and subsequent tsunamis. An important characteristic of subduction zones is the dip angle of the Wadati-Benioff seismic focal zone. Variations in this parameter are observed around the perimeter of the Pacific Ring [*Lallemand et al.*, 2005].

Off the western coast of South America, subduction beneath the continental lithosphere occurs at relatively shallow angles, typically 10°–30°. In contrast, the subduction zones near the Aleutian Islands, the Kuril–Kamchatka Arc, Japan, Indonesia, and New Zealand are characterized by dip angles reaching 45°–60° and greater. This is due to the greater age and, consequently, higher density of the oceanic lithosphere in the western Pacific Ocean [*Jarrard*, 1986]. Steep subduction angles give rise to distinct types of volcanism and focal mechanisms. The contact zone between the Pacific and North American plates along the western margin of the North American continent is predominantly characterized by a transform fault. This results in a lower level of seismicity and a more scattered distribution of earthquake epicenters on the mainland, in contrast to the Wadati-Benioff seismic focal zone.

1.1. Strongest Earthquakes of the Pacific Ring of Fire in the Second Half of the 20th and Early 21st Centuries

Within the Pacific Seismic Belt, earthquakes of all magnitudes, including the strongest ones, occur tens of times more frequently than outside its boundaries [*Fedotov*, 2005]. Figure 1 shows the epicenters of earthquakes with $M_W \geq 8.0$ [*Di Giacomo et al.*, 2018; *International Seismological Centre*, 2026] in the Pacific region. In the context of the present study, we will examine in greater detail the events with $M_W \geq 8.5$ that have occurred since 1952, the year of the previous megathrust earthquake in Kamchatka. In Figure 1, the epicenters of considered earthquakes with $M_W \geq 8.5$ are marked in green.

The Severo-Kurilsk earthquake with $M_W = 9.0$ [*Kanamori*, 1977] is one of the strongest seismic events within the Pacific Ring of Fire. It occurred on November 5, 1952, at a distance of 100–150 km southeast of the southern tip of the Kamchatka Peninsula. The earthquake did not cause severe damage on land. The only minor damage was reported from the Kronotsky Peninsula in Kamchatka to the Northern Kuril Islands [*Fedotov*, 1962, 1965]. However, the earthquake caused a catastrophic tsunami that practically washed the town of Severo-Kurilsk on Paramushir Island into the ocean [*Nikonov*, 2006]. According to [*Johnson and Satake*, 1999], the length of the coseismic rupture in the subduction zone was 600 km.

The Andreanof Islands earthquake of March 9, 1957, with $M_W = 8.6$ [*Johnson et al.*, 1994], occurred south of the Andreanof Islands (a subgroup of the Aleutian Islands) and caused localized damage on Adak Island. This earthquake produced the longest aftershock zone of any instrumentally recorded event, stretching 1,200 km [*Johnson et al.*, 1994].

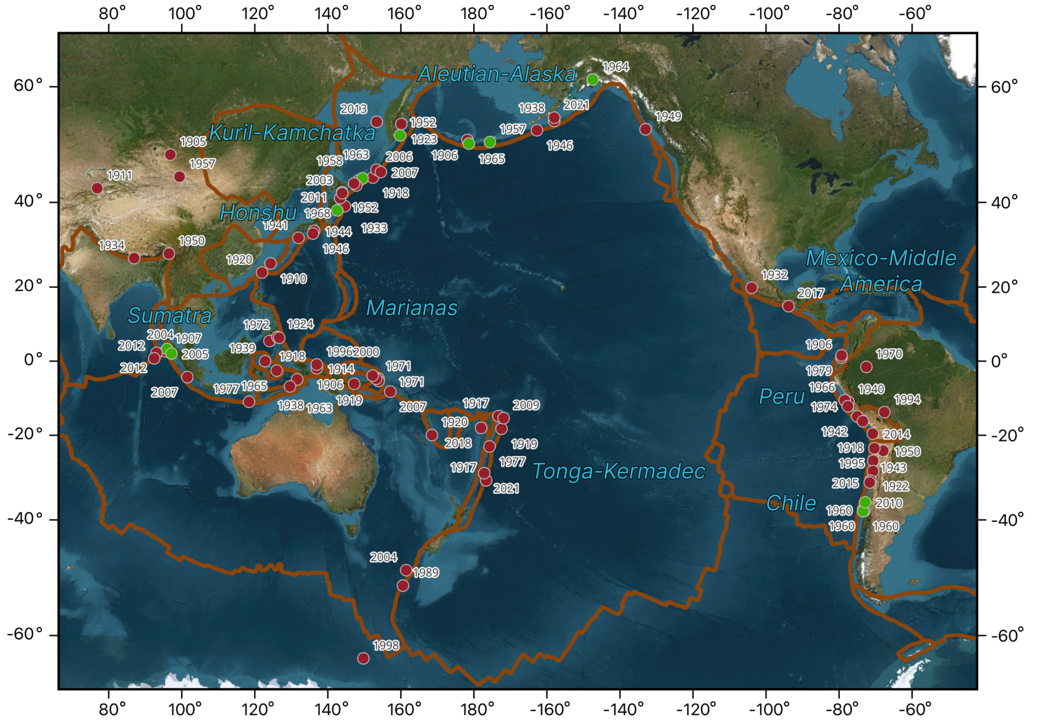

Figure 1. Map of the earthquake epicenters with $M_W \geq 8.0$ from the ISC-GEM catalog for 1904–2021 [*Di Giacomo et al.*, 2018; *International Seismological Centre*, 2026] in the Pacific Seismic Belt region.

The magnitude of this event was estimated at $M_W = 9.1$ in [*Kanamori*, 1977]. However, it was later shown in [*House et al.*, 1981] that the seismic moment had been miscalculated because the earthquake rupture did not encompass the eastern part of the aftershock zone. The earthquake was followed by tsunami waves up to 15–16 meters high that struck the coast of the Aleutian Islands, causing significant damage to Unimak, Adak, and Unalaska [*Johnson et al.*, 1994]. The tsunami was recorded by tide gauges across the Pacific Ocean, with waves reaching San Diego Bay, the coasts of Chile, El Salvador, and Japan, and also causing destruction in Hawaii.

On May 22, 1960, off the coast of Chile, the Great Chilean (Great Valdivia) earthquake with $M_W = 9.5$ occurred. It is considered the most powerful instrumentally recorded seismic event in history [*Kanamori*, 1977]. The earthquake was followed by a series of powerful aftershocks. The mainshock was followed by a massive tsunami, whose waves caused destruction and casualties in Chile, as well as along the coasts of Japan, Hawaii, the Philippines, and New Zealand. The length of the coseismic rupture generated by the earthquake at the southern end of the Nazca Plate, which subducts beneath the South American Plate along the Peru-Chile Trench, reached up to 1,000 km [*Cifuentes*, 1989]. Note that 33 hours prior to the Great Chilean earthquake, approximately 200 km away, an earthquake with $M_W = 8.1$ struck the Concepción region in Chile [*Ojeda et al.*, 2020].

The Urup earthquake with $M_W = 8.5$ [*Kanamori*, 1977] occurred on October 13, 1963, off the coast of Urup Island (Southern Kurils). The earthquake and the subsequent tsunami, which had moderate wave heights, did not cause significant damage to the islands of the Southern Kurils. One day before the main event, a foreshock with $M_s = 6.7$ was recorded. A major aftershock with $M_s = 7.3$ occurred on October 20 on the oceanic trench side relative to the epicenter of the mainshock. According to [*Beck and Ruff*, 1987], the coseismic fault of the earthquake, with a length of 245 km, was characterized by complex geometry and several asperity zones. This was the cause for the release of such a high seismic moment.

The Great Alaska earthquake with $M_W = 9.2$ [*Kanamori*, 1970, 1977] occurred on March 27, 1964. Its epicenter was located in the Gulf of Alaska, 120 km east of Anchorage.

The earthquake itself did not cause numerous casualties and widespread structural damage, although soil liquefaction was observed in Anchorage. A submarine landslide triggered by the earthquake led to the destruction of the port of Valdez. The earthquake initiated a powerful tsunami that struck the coasts of Alaska, Canada, and the United States. Its waves were observed along the coasts of Hawaii, Japan, and Chile. The length of the coseismic rupture generated by the earthquake in the subduction zone of the Pacific Plate beneath the North American Plate exceeded 600 km [*Kanamori*, 1970].

The Rat Islands are part of the Aleutian Island Arc. They are situated above the subduction zone of the Pacific Plate beneath the North American Plate. An earthquake that occurred here on February 4, 1965, with $M_W = 8.7$ [*Kanamori*, 1977], produced a coseismic rupture 600 km long along the western extremity of the Aleutian Islands. In [*Beck and Christensen*, 1991], temporal and spatial heterogeneities of the rupture were identified. They were localized at three asperities corresponding to the Rat Islands, Buldir, and Near Islands tectonic blocks.

In 2004 (December 26) and 2005 (March 28), the two strongest earthquakes occurred in the Indian Ocean in the subduction zone of the Indo-Australian Plate beneath the southeastern part of the Eurasian Plate. The magnitude of the first, which occurred off the northwest coast of Sumatra and ranks among the top three strongest earthquakes in the history of seismic observations, was estimated at $M_W = 9.1$–9.3 according to various sources [*Khan and Gudmundsson*, 2005; *Lay et al.*, 2005]. The epicenter of the second, with $M_W = 8.6$, was located 160 km southeast of the epicenter of the first [*Konca et al.*, 2007]. The length of the fault rupture generated by the 2004 earthquake reached 1,300 km, stretching from northwestern Sumatra to the Andaman Islands. The total length of the rupture from both earthquakes in the subduction zone of the Indo-Australian Plate beneath the southeastern Eurasian Plate amounted to 1,600 km [*Lay et al.*, 2005]. The 2004 event triggered the deadliest tsunami in history. This catastrophe was exacerbated by the high population density of Southeast Asian countries and the absence of a tsunami warning system in the Indian Ocean.

On February 27, 2010, an earthquake with $M_W = 8.8$ [*Delouis et al.*, 2010; *Moreno et al.*, 2012; *Vigny et al.*, 2011] struck the coast of central Chile, approximately 360 km southwest of Santiago. This was the strongest event in the region since the Great Chilean earthquake The rupture that occurred in the subduction zone of the Nazca Plate beneath the South American Plate was 500 km long. The subsequent tsunami, with wave heights up to 10 meters, caused severe damage to the Chilean coast and the Juan Fernández Islands.

On March 11, 2011, the Tohoku earthquake with $M_W = 9.0$ [*Simons et al.*, 2011] struck the eastern coast of Japan. It was followed by one of the most productive aftershock sequences in the history of instrumental observations [*Vorobieva et al.*, 2022]. The length of the fault rupture from the earthquake in the subduction zone, where the Pacific Plate subducts beneath the Okhotsk Plate at a relatively gentle dip angle, was 400 km [*Ozawa et al.*, 2011]. At the same time, the amplitude of coseismic displacements along the fault in the Japan Trench locally exceeded 50 m. In [*Simons et al.*, 2011], this is explained by the role of stress concentration zones or asperities, slow earthquakes, and non-volcanic tremors in the transition regions of subduction zones. Such significant fault displacement triggered a devastating tsunami that struck Japan and led to the Fukushima Daiichi nuclear disaster. Over 400 km^2 of Japan's coastal territory was inundated, and the maximum recorded run-up height in the city of Miyako (Iwate Prefecture) reached 40.5 m [*Mori et al.*, 2011]. The tsunami waves reached the coasts of North and South America, Hawaii, and even Antarctica.

The list of the ten strongest megathrust earthquakes in the world [*Di Giacomo et al.*, 2018; *Storchak et al.*, 2013, 2015] includes 8 of the 10 events above and clearly shows that the Pacific Seismic Belt is the most seismically hazardous region on Earth. In the second half of the 20th century, the works on pattern recognition of earthquake-prone areas by I. M. Gelfand, V. I. Keilis-Borok, A. D. Gvishiani, Al. An. Soloviev, V. G. Kosobokov, Sh. A. Guberman, E. Ya. Rantsman, L. Knopoff, F. Press, and others [*Gelfand et al.*, 1976;

Gvishiani and Soloviev, 1981; *Gvishiani et al.*, 2020, 1978, 1980, 1984, 1982] made a major contribution to the study of its seismic regime. In the 21st century, for specific regions of the Pacific Ring of Fire, new insights into areas prone to the strongest earthquakes were obtained by A. D. Gvishiani, B. A. Dzeboev, and S. M. Agayan using modern pattern recognition methods [*Dzeboev et al.*, 2018a, 2021, 2018b; *Gvishiani et al.*, 2013a; *Gvishiani et al.*, 2013b, 2016]. The FCAZ (Formalized Clustering And Zoning) method, developed by A. D. Gvishiani and B. A. Dzeboev, made it possible to assess seismic hazard based on initial data without relying on morphostructural zoning.

1.2. Long-Term Earthquake Prediction for the Pacific Ring of Fire

The earliest research on long-term earthquake prediction for various segments of the Pacific seismic ring was conducted by prominent seismologists S. A. Fedotov (USSR/Russia), K. Mogi (Japan), L. R. Sykes (USA), J. A. Kelleher (USA), S. P. Nishenko (USA), W. R. McCann (Puerto Rico/USA), and others [*Fedotov*, 1965; *Kelleher*, 1970, 1972; *McCann et al.*, 1979; *Mogi*, 1968, 1969]. These studies were based on the seismic gap theory that was proposed almost simultaneously by S. A. Fedotov, K. Mogi, and L. R. Sykes. However, priority in conducting this research belongs to S. A. Fedotov [*Fedotov*, 1965]. The aforementioned researchers identified the main seismic gaps for several major plate boundaries in the Pacific Ring regions. Subsequently, these gaps were "filled" by coseismic ruptures from the strongest earthquakes [*McCann et al.*, 1979]. It should also be noted that at different stages of research, the seismic gap theory was subject to criticism [*Kagan and Jackson*, 1991; *Rong et al.*, 2003].

In [*Nishenko*, 1991], S. P. Nishenko divided the Pacific Ring of Fire into 96 segments, for which predictions were made for 5-, 10-, and 20-year periods. For instance, for a 10-year period, high seismic potential was assigned to 11 segments, while for a 20-year period, this number increased to 30 segments.

An outstanding contribution to research on long-term earthquake prediction and the assessment of time-dependent seismic hazard for segments of the Pacific Seismic Belt belongs to full member of the Russian Academy of Sciences (1992) and corresponding member of the USSR Academy of Sciences (1970) Sergey A. Fedotov [*Fedotov*, 2005]. He obtained fundamental results on long-term earthquake prediction for the Kuril–Kamchatka subduction zone of the Pacific Plate under the Okhotsk Plate [*Schellart et al.*, 2003], as part of the Pacific Ring [*Fedotov*, 1965, 1967, 1968].

Within the Kuril–Kamchatka Arc, east of Petropavlovsk-Kamchatsky, an earthquake with $M_W = 8.8$ occurred on July 29, 2025. It ranks among the ten strongest earthquakes instrumentally recorded since 1900 [*USGS*, 2025]. The distance between its epicenter and the epicenter of the 1952 Severo-Kurilsk earthquake is 30 km. The 2025 event was preceded by 50 seismic events with $M \geq 5.0$, including the earthquake with $M_W = 7.4$ that occurred on July 20, 2025. Within the first 24 hours after the mainshock, 24 aftershocks with $M \geq 5.0$ were recorded, including two with $M_W = 6.8$ and $M_W = 6.2$ [*Chebrov et al.*, 2026]. The strongest aftershocks occurred on September 13 and 18 with $M_W = 7.4$ and $M_W = 7.8$ respectively [*Chebrov*, 2025]. A detailed description of the Kamchatka megathrust earthquake of July 29, 2025 is provided in [*Chebrov*, 2025; *Chebrov et al.*, 2026; *Konovalov et al.*, 2026; *Mikhailov et al.*, 2025a].

Unlike the aforementioned megathrust earthquakes that occurred earlier in the 20th and 21st centuries, the Kamchatka earthquake of July 29, 2025 became the first megathrust earthquake in history to cause no direct human casualties or structural damage. This outcome was due in part to timely seismic retrofitting of buildings and infrastructure in the Kuril–Kamchatka region, combined with other preventive measures. These actions were initiated and directly planned with the active participation of Sergey A. Fedotov, who served as the Director of the Institute of Volcanology and Seismology of the Far Eastern Branch of the Russian Academy of Sciences from 1971 to 2004. These measures were based on the results of his research on the seismic regime and seismic hazard assessment of the Kuril–Kamchatka Arc.

The present article is dedicated to a contemporary reassessment of results obtained by S. A. Fedotov regarding the long-term earthquake prediction for the Kuril–Kamchatka Arc in light of the Kamchatka megathrust earthquake of July 29, 2025, which occurred six years after Fedotov passed away.

2. Long-Term Earthquake Prediction by S. A. Fedotov for the Kuril–Kamchatka Arc

2.1. Development of the Method

The beginning of research on long-term earthquake prediction for the Kuril–Kamchatka Arc by S. A. Fedotov can be considered 1957 [*Fedotov*, 2008, 2013; *Fedotov et al.*, 1969; *Gordeev et al.*, 2013]. At that time, the expeditionary team led by him, as part of detailed seismological studies in the Kuril Islands and Kamchatka, expanded the seismic network on the islands of Iturup, Kunashir, and Shikotan [*Fedotov*, 1987, 2005]. This made it possible to record both the Iturup earthquake of November 6, 1958, with $M = 8.2$ [*Fedotov*, 1962; *Fedotov et al.*, 1969], its foreshocks and aftershock swarm (1958–1964) [*Fedotov*, 1969], and the Urup earthquake with $M = 8.1$, which occurred on October 13, 1963, near the source of the Iturup event. The study of the relationship between the sources of the strongest earthquakes and the processes occurring within them led Dr. S. A. Fedotov to the fundamental concepts of his long-term earthquake prediction method [*Fedotov*, 2005, 2008].

The main stages of the development, evolution, and application of the method developed by S. A. Fedotov for the Kuril–Kamchatka Island Arc are described in [*Fedotov*, 1965, 1967, 1968, 1969, 2005; *Fedotov et al.*, 1970, 1972, 1977]. The seismic region he studied (the Kuril–Kamchatka Trench) extends for 2,000 km and is 150–200 km wide, stretching from Hokkaido Island (Japan) along the Kuril Islands and the Pacific coast of the Kamchatka Peninsula, ending at the intersection with the Aleutian subduction zone [*Fedotov*, 2005].

In 1965, S. A. Fedotov studied the distribution pattern of strong earthquakes in Kamchatka, the Kuril Islands, and northeastern Japan, which continues the Kuril–Kamchatka seismic zone [*Fedotov*, 1965]. He considered 43 events with magnitudes $M \geq 7.75$ [*Fedotov*, 1972] and depth $h < 100$ km that occurred between 1896 and 1964. It was revealed that within the Kuril–Kamchatka zone, earthquakes that occurred between 1904 and 1963 were grouped into two time periods (1915–1924 and 1952–1963), separated by a 28-year period of quiescence. It was shown that the observed combinations of periods of seismic activity and quiescence are least likely under the assumption of a random distribution of earthquakes in time. This argued in favor of the non-randomness and interconnectedness of events, as well as the possibility of their long-term prediction.

Analysis of the graph of seismic energy release and the spatial distribution of source areas of earthquakes in the region allowed S. A. Fedotov to find the relationship between events and establish that earthquake sources tend not to overlap each other (Figure 2). This made it possible in 1965 to construct a long-term prediction for areas of future strong earthquakes as zones between the sources of earthquakes with $M \geq 7.75$ (Figure 2) that occurred between 1904 and 1963 [*Fedotov*, 1965]. Such probable areas of the next strongest earthquakes were called seismic gaps [*Fedotov*, 2005].

In 1968, S. A. Fedotov introduced the fundamental concept of the seismic cycle as the course of the seismic regime at a given area in the time interval between two maximum magnitude earthquakes occurring at approximately the same location [*Fedotov*, 1968]. Based on the analysis of time intervals between catastrophic earthquakes and the assumption of preserving the rates of area coverage of the region by earthquake sources, he derived an estimate for the average duration of the seismic cycle in the Pacific focal zone off the coasts of Kamchatka, the Kuril Islands, and Japan – 140 ± 60 years [*Fedotov*, 2005].

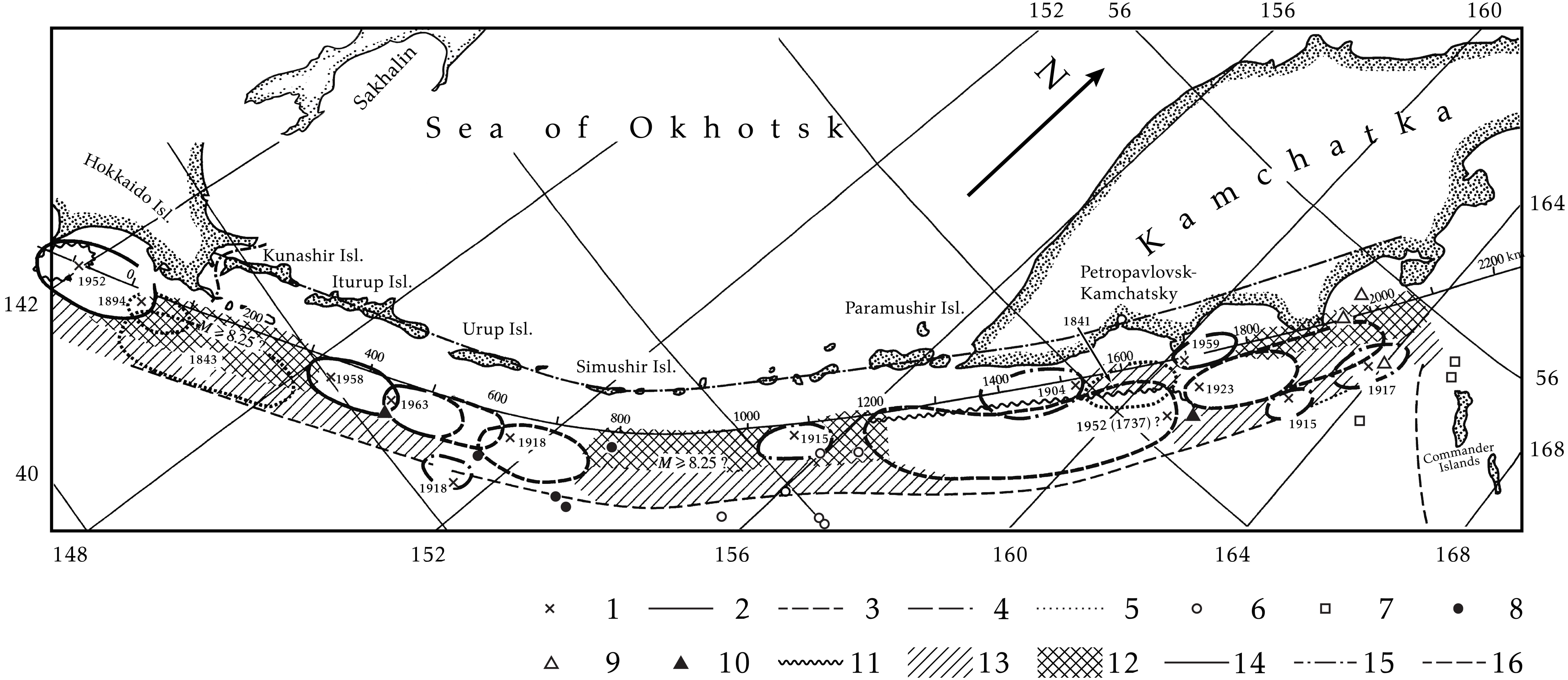

Figure 2. Source areas of Kuril–Kamchatka earthquakes of 1904–1963 with $M \geq 7.75$ and probable areas of future earthquakes with $M \geq 7.75$ (from [*Fedotov*, 1965, 2005]): 1 – instrumental epicenters of earthquakes with $M \geq 7.75$; 2 – boundaries of source areas of earthquakes with $M \geq 7.75$; 3 – uncertain parts of boundaries or possible variants of source area boundaries; 4 – possible source areas; 5 – presumed source areas of the strongest earthquakes of the 19th century; 6 – aftershocks of the earthquake of May 1, 1915; 7 – aftershocks of the earthquake of January 30, 1917; 8 – aftershocks of the earthquake of September 7, 1918; 9 – aftershocks of the earthquake of February 3, 1923; 10 – strong foreshocks of the 1923 and 1963 earthquakes; 11 – boundaries of tsunamigenic areas; 12 – most probable areas of the next earthquakes with $M \geq 7.75$; 13 – less probable locations of the next earthquakes with $M \geq 7.75$; 14 – distance reference line along the Pacific focal zone outcrop to the ocean floor; 15 – axes of deep-sea trenches; 16 – axis of the Kuril–Kamchatka volcanic belt.

2.2. Cycles of Seismic Activity $A_{10}(t)$ and Seismic Energy Release $D(t)$

In 1968, in [*Fedotov*, 1968], based on the combined data of ten source areas, S. A. Fedotov considered a typical cycle of change in seismic activity $A_{10}(t)$ (the number of 10th energy class earthquakes [*Fedotov*, 1972] per year per 1,000 km^2 area) in one area during the time period between two catastrophic earthquakes in the Kuril–Kamchatka region and Japan.

Analysis of the graph $A_{10}(t)$ (Figure 3) reveals three intervals in the seismic cycle: the aftershock period (Stage I), the period of long-term regime stabilization (Stage II), and the foreshock period (Stage III). The author noted that the average duration of aftershocks for catastrophic earthquakes is 15 years. During this time the values $A_{10}(t)$ decrease from several thousand (right after the event) to 1.0–2.0. The duration of the stabilization period is approximately 110 years (for a 140-year cycle) with $A_{10}(t) \approx 1.0$. On average, 15 years before the next catastrophic earthquake, the values $A_{10}(t)$ begin to increase, reaching 3.5 before the event (Figure 3) [*Fedotov*, 1968, 2005].

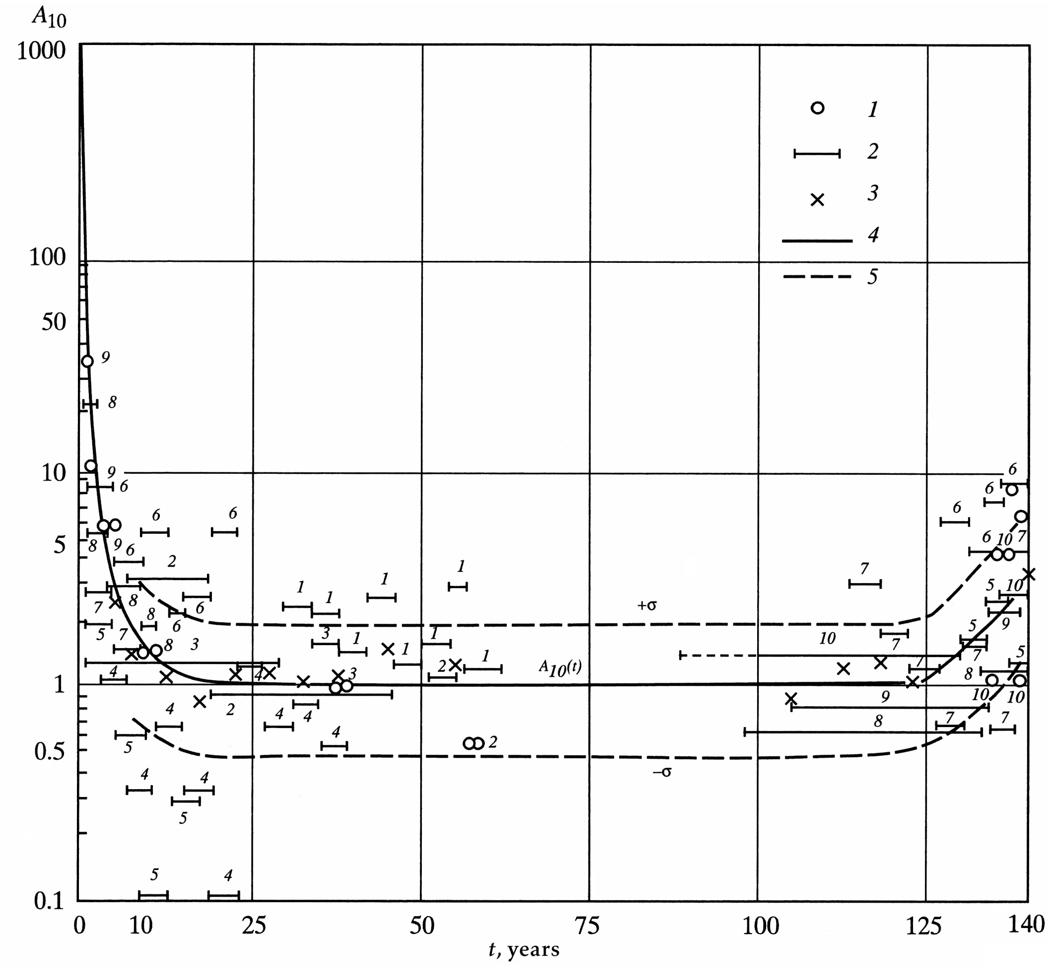

Figure 3. Cycle of seismic activity $A_{10}(t)$ in the Pacific focal zone off the coasts of Kamchatka, the Kuril Islands, and northeastern Japan (from [*Fedotov*, 1968, 2005]): 1 – average annual A_{10} values obtained from detailed seismological studies; 2 – calculated A_{10} values [*Fedotov*, 1968]; 3 – mean geometric A_{10} values in time intervals of the cycle lasting 5 years or more; 4 – averaged graph of $A_{10}(t)$ change during the cycle; 5 – boundaries of $\sigma(\lg A_{10}) = \pm 0.3$. The numbers on the graph correspond to earthquake numbers considered in [*Fedotov*, 1968].

By calculating the average annual values of the released seismic energy, it was concluded that seismic activity and earthquake recurrence under the upper part of the continental slope of the deep-sea trench in the Kuril–Kamchatka region are twice as high as under the lower part of the slope [*Fedotov*, 1968].

In [*Fedotov*, 1968], the concept of a measure of seismic energy release over time t at a given location was introduced as $D(t) = E_2(t)/E_1$, where $E_2(t)$ J/10^3km$^2\cdot$ year is the specific seismic energy of earthquakes that occurred in the region over time t; E_1 is the seismic energy released in the region on average per year per area 10^3km^2 and approximately corresponds to an earthquake with $M = 6.25$.

In contrast to $A_{10}(t)$, which characterizes the activity of weak earthquakes during the seismic cycle, $D(t)$ shows the distribution features of strong earthquakes in this cycle. Analysis of the $D(t)$ graph constructed on data from nine source areas of catastrophic earthquakes at different stages of the cycle (Figure 4) showed the following. In the first year after the event $D(t) \geq 100$, i.e., energy accumulated over 100 or more years is released. From the second year, a decrease occurs from $D \approx 1.0$, reaching $D \approx 0.1$ after 10–15 years by the end of the aftershock sequence. Then, during the 100-year (with a 140-year cycle) stabilization period of A_{10}, the value of D gradually decreases to 0.01. This means that the energy and number of strong earthquakes slowly decrease and reach a minimum approximately 100 years after the catastrophic earthquake. The number of strong earthquakes and the energy released begin to increase about 30 years before the next catastrophic earthquake. Moreover, in the last 5 years before it $D \approx 0.1$, as at the end of the aftershock stage (Figure 4) [*Fedotov*, 1968, 2005].

From knowledge of $A_{10}(t)$ and $D(t)$ at different stages of the seismic cycle for average source areas (15,000 km^2) and 5-year time intervals, the magnitudes of expected earthquakes $M(A_{10})$ and the most probable magnitudes of the strongest earthquakes $M(D)$ were calculated [*Fedotov*, 1968]. Their analysis showed that the beginning of the aftershock stage (2–10 years of the cycle) and the end of the foreshock stage (last 5–10 years of the cycle) are characterized by strong events with $M \geq 6.75$–7.0. During the stabilization stage, the most probable magnitudes of the strongest earthquakes occurring once every five years gradually decrease from 6.75 ± 0.5 to 6.25 ± 0.5 [*Fedotov*, 1968, 2005].

Based on the analysis of activity A_{10} determined during the stabilization stage, S. A. Fedotov introduced rules for establishing boundaries between areas with different long-term seismicity levels. The author also estimated the differences in seismicity levels in these areas [*Fedotov*, 1968, 2005].

Analysis of $M(D)$ showed that during years 2 to 6 of the cycle, stresses capable of causing events with a magnitude of up to 7.25 persist.

Combined with estimates of the average annual accumulation of seismic energy, this enabled tentative predictions of future accumulation rates ($E(t)\frac{\text{J}}{5\cdot 10^3\text{km}^2} \approx [280 + 0.3 \cdot t^2 \text{ years}] \cdot 10^{14}$, where t is the cycle duration in years) and, accordingly, the maximum possible earthquake magnitudes [*Fedotov*, 1968, 2005].

In 1980, in [*Fedotov et al.*, 1980], based on seismicity data in the sources of earthquakes with $M \geq 7.75$ from 1952–1978, the $A_{10}(t)$ cycle was verified and refined (Figure 5). It turned out to be close to the previously constructed one (Figure 3) [*Fedotov*, 1968, 2005]. As can be seen from comparing the figures, the stable regime stage (II) lasting 100–110 years is still clearly identified, and the foreshock stage (III) lasting 15–20 years is less reliably distinguished. Among the differences, it should be noted that the value of seismic activity at stage II is $A_{10} = 1.25$ (previous value was $A_{10} = 1.0$ [*Fedotov*, 1968, 2005]). The standard deviation of A_{10} from the average graph decreased from $\sigma(\lg A_{10}) = \pm 0.3$ [*Fedotov*, 1968, 2005] (corresponds to a change in activity by a factor of two in both directions from the average value) to $\sigma(\lg A_{10}) = \pm 0.18$ [*Fedotov*, 2005; *Fedotov et al.*, 1980] (corresponds to a change in activity by a factor of 1.5). This change in variance is explained by greater homogeneity and completeness of the new data [*Fedotov et al.*, 1980]. At the end of the cycle, at stage III, a significant increase in seismic activity occurs (Figure 5) [*Fedotov*, 2005; *Fedotov et al.*, 1980].

The $D(t)$ cycle was verified and refined (Figure 6) based on seismicity data in earthquake sources for 1904–1978 [*Fedotov et al.*, 1980]. As in the case of $A_{10}(t)$, three stages of the seismic cycle are identified. Among the differences from the $D(t)$ graph constructed in [*Fedotov*, 1968, 2005] (Figure 4) are the disappearance of the minimum at the end of

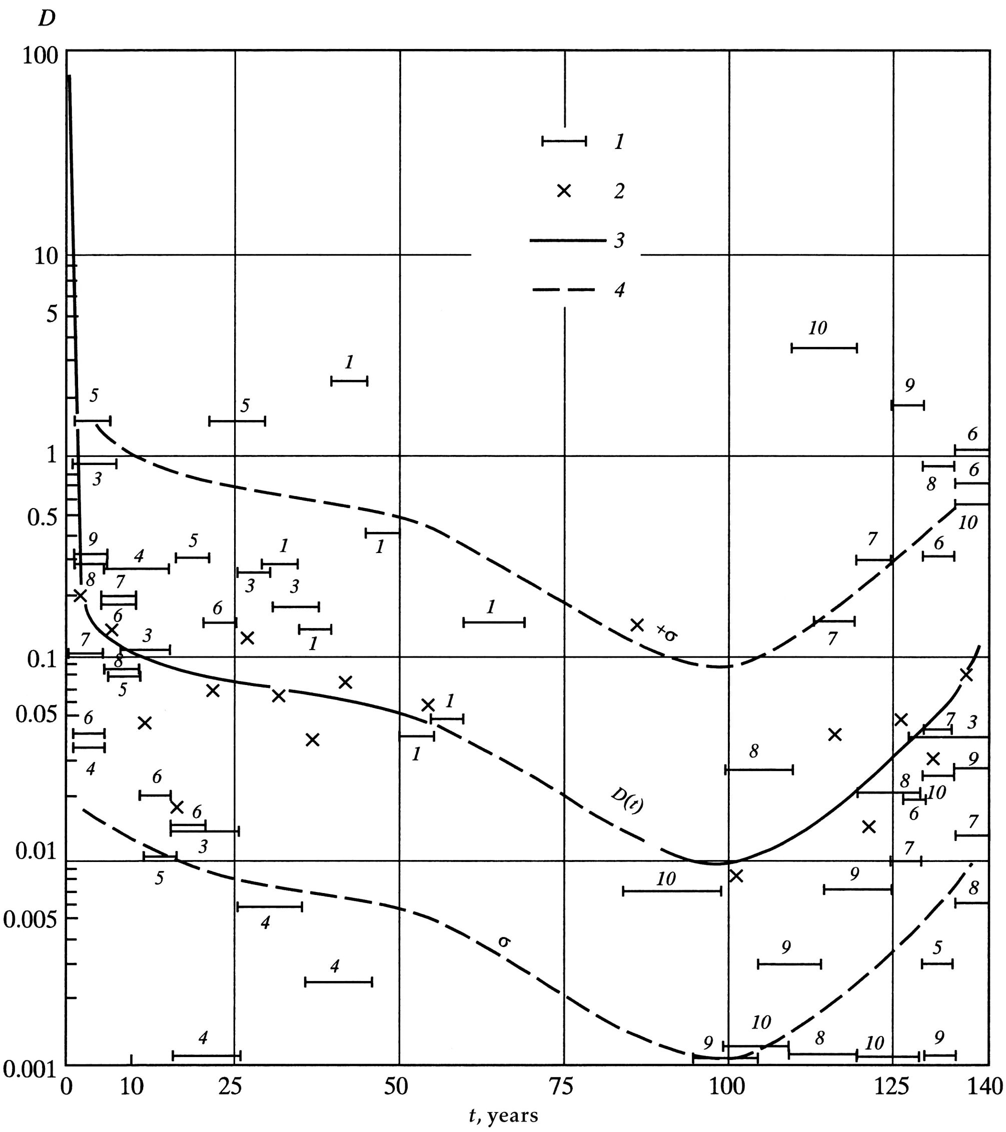

Figure 4. Cycle of seismic energy release $D(t)$ in the Pacific focal zone off the coasts of Kamchatka, the Kuril Islands, and northeastern Japan (from [*Fedotov*, 1968, 2005]): 1 – average over 5 years or more values of D in the source areas of Kuril–Kamchatka and Japanese earthquakes with $M \geq 7.75$; 2 – mean geometric values of D in 5-year intervals of the seismic cycle; 3 – averaged graph of $D(t)$ change during the cycle; 4 – boundaries of $\sigma(\lg D) = \pm 1.0$. The numbers on the graph correspond to earthquake numbers considered in [*Fedotov*, 1968].

stage II and a decrease in the standard deviation from $\sigma(\lg D) = \pm 1.0$ [*Fedotov*, 1968, 2005] (corresponds to a change in D by a factor of ten in both directions from the average value) to $\sigma(\lg D) = \pm 0.72$ [*Fedotov*, 2005; *Fedotov et al.*, 1980] (corresponds to a change by a factor of five). The regime of seismic energy release at the aftershock and foreshock stages remained mainly the same [*Fedotov*, 2005; *Fedotov et al.*, 1980].

In 2008, S. A. Fedotov, in [*Fedotov et al.*, 2008], carried out a new verification and refinement of the parameters $A_{10}(t)$ and $D(t)$ that are used to calculate the prediction values. The leading prognostic parameter is $A_{10}(t)$. The $A_{10}(t)$ cycle was refined using data from 17 source areas for the period 1904–2006. Among the refined values of $A_{10}(t)$, the following should be noted: the average values in the second half of stage II of the cycle are $A_{10}(\mathrm{II}, t = 70-120 \text{ years}) = 1.15$; the average values in the last 10 years of stage III of the cycle are $A_{10}(\mathrm{III}, t = 130-140 \text{ years}) = 2.17$; and the average values in the last 5 years of stage III of the cycle are $A_{10}(\mathrm{III}, t = 135-140 \text{ years}) = 2.62$. It was established that $A_{10}(t)$

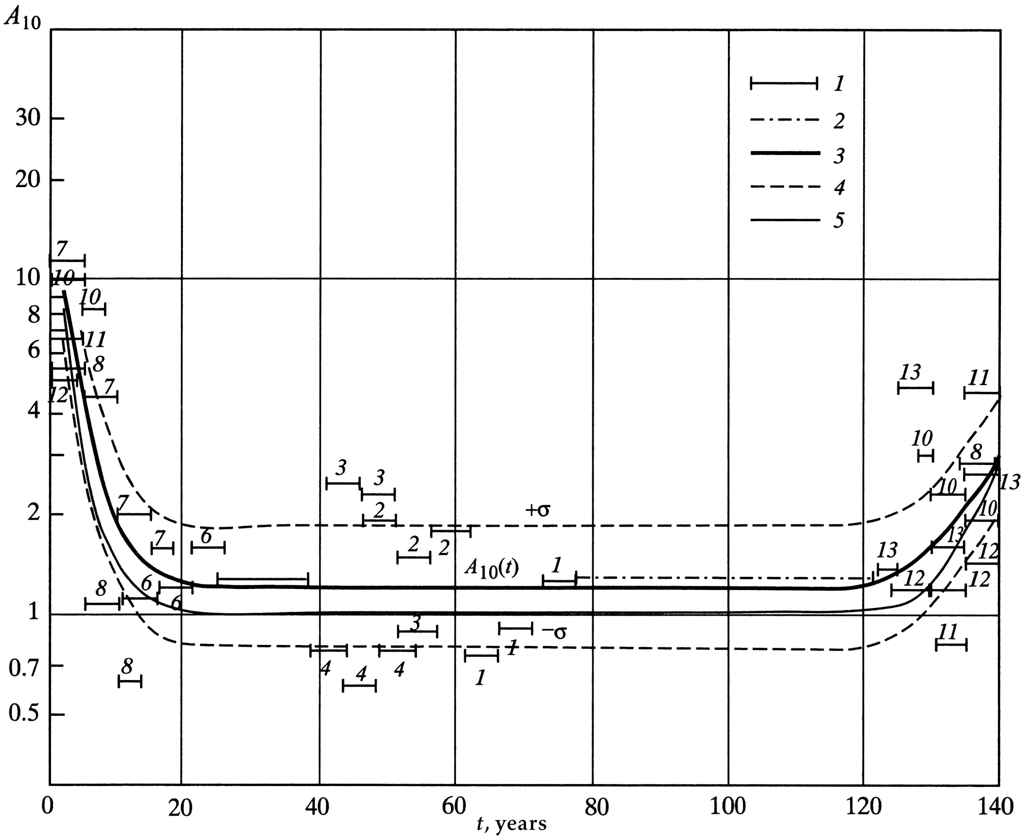

Figure 5. Cycle of seismic activity $A_{10}(t)$ in the Pacific focal zone off the coasts of Kamchatka, the Kuril Islands, and northeastern Japan (from [*Fedotov*, 2005; *Fedotov et al.*, 1980]): 1 – average seismic activity values for 5 years (numbers correspond to earthquake numbers considered in [*Fedotov et al.*, 1980]); 2 – average annual A_{10} values determined from annual seismic activity maps of Kamchatka; 3 – averaged graph of A_{10} change during the cycle; 4 – boundaries of standard deviation $\sigma(\lg A_{10}) = \pm 0.18$; 5 – graph of $A_{10}(t)$ from [*Fedotov*, 1968, 2005].

increases, on average, by a factor of 1.9 during the last 10 years of the cycle and by a factor of 2.3 during the last 5 years of the cycle. It was also noted that the value A_{11} (see text below) [*Fedotov et al.*, 2007] increases more slowly than A_{10} but does so monotonically over the last 40 years of the cycle. Thus, estimates of A_{11} over three five-year intervals enhance the reliability of identifying stage III of the cycle [*Fedotov et al.*, 2008].

2.3. The First Long-Term Earthquake Prediction (1965–1985)

The identified systemic regularities in the distribution of strong earthquake sources, the properties of the seismic cycle, and the magnitude of natural seismicity fluctuations enabled S. A. Fedotov, in 1968, to construct for the first time a long-term earthquake prediction for the Kuril–Kamchatka arc. The prediction was constructed for 13 large segments of a 100-km-wide strip extending along the upper part of the continental slope of the deep-water trench for the time periods 1965–1970, 1971–1975, 1976–1980, and 1981–1985 [*Fedotov*, 1968, 2005].

For each segment, the prediction included the positions of the seismic gaps, the stage of the seismic cycle, the relative hazard of the seismic gaps, the probable values of seismic activity A_{10}, the most probable magnitude of the strongest earthquake $M(D)$ with probabilities of 0.8, 0.5, and 0.15, and the maximum possible earthquake magnitudes $M_{\max}$ [*Fedotov and Chernyshev*, 2002]. Among the 13 segments, those within which the next earthquake with $M \geq 7.75$ was most probable were identified, as well as those in which such an earthquake was unlikely in the coming years. Note that as early as 1968

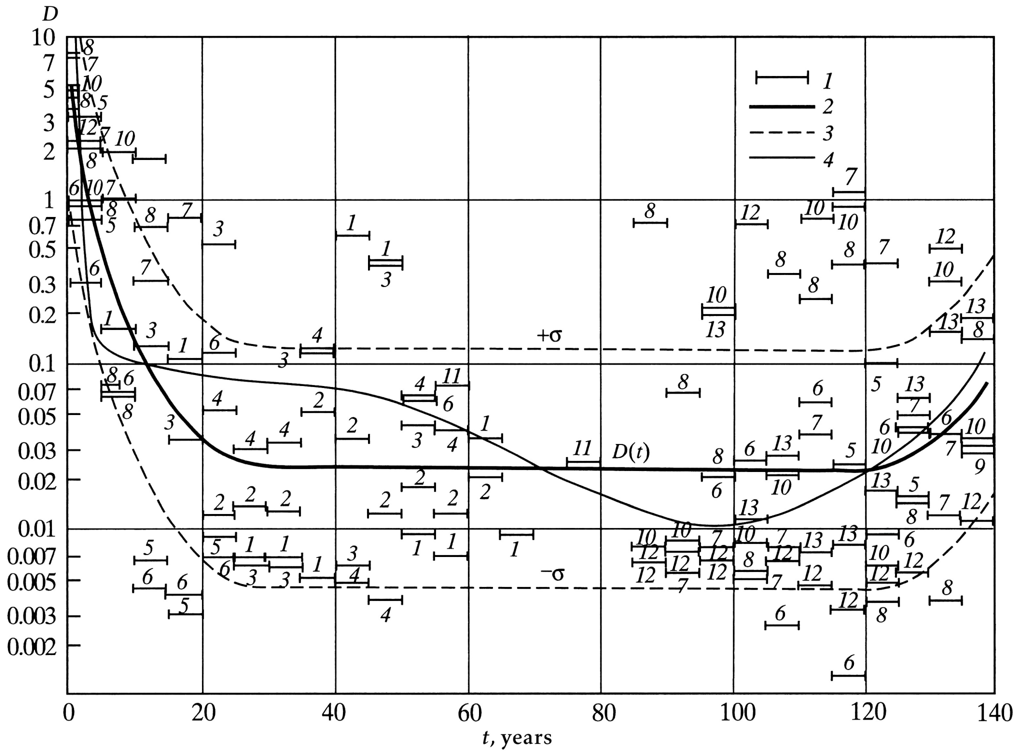

Figure 6. Cycle of seismic energy release $D(t)$ in the Pacific focal zone off the coasts of Kamchatka, the Kuril Islands, and northeastern Japan (from [*Fedotov*, 2005; *Fedotov et al.*, 1980]): 1 – average for 5 years values of D in the source areas of earthquakes with $M \geq 7.75$ (numbers correspond to earthquake numbers considered in [*Fedotov et al.*, 1980]); 2 – averaged graph of change during the cycle; 3 – boundaries of standard deviation $\sigma(\lg D) = \pm 0.72$; 4 – graph of $D(t)$ from [*Fedotov*, 1968, 2005].

[*Fedotov*, 1968], the prediction for the region containing the source areas of the 1952 and 2025 earthquakes was given in two variants – for the western and eastern parts of the segment of the considered strip.

In subsequent years, the predictions were systematically refined as new data on earthquakes in the region became available. The predictions were regularly verified. The first verification, carried out in 1974 [*Fedotov*, 1974], demonstrated the success of the prediction made for 1965–1970 [*Fedotov*, 1968]. The earthquake near Shikotan Island on August 12, 1969 with $M = 8.0$ occurred in the area where such events had been expected according to the prediction. With regard to the prediction of A_{10} and the magnitudes of the anticipated earthquakes (with a probability of 0.8), it should be stated that the prediction was confirmed for 6 of the 7 segments for which it had been constructed, and all earthquakes with $M \geq 7.5$ occurred where they had been predicted as possible in 1965–1970.

Following the 1969 earthquake near Shikotan Island and the changes it introduced into the seismic situation, the prediction for 1971–1975 was adjusted [*Fedotov*, 1974, 2005]. For each segment, the stage of its seismic cycle was refined. If no event with $M \geq 7.75$ had occurred within a segment since 1904, it was assigned stage III.

Taking into account the mean values of activity A_{10} and seismic energy in conventional units D, characteristic for different stages of the cycle, as determined in [*Fedotov*, 1968, 2005], new probabilistic parameters $P(A_{10})$ and $P(D)$ were introduced in [*Fedotov*, 1974]:

- $P(A_{10})$ – the probability that the value of A_{10}, averaged over the preceding five years, exceeds the level of A_{10} that exists in stage II of the seismic cycle (the prolonged stage of seismic energy accumulation);

- $P(D)$ – the probability that the value of D, averaged over the preceding five years, exceeds the level of D observed in stage II of the seismic cycle.

S. A. Fedotov noted that the smaller the product $P(A_{10}) \cdot P(D)$, the greater the probability that the considered segment is passing through stage III of foreshocks.

Using knowledge of the current stage of the seismic cycle, the values of $P(A_{10}) \cdot P(D)$, and the assumption of a 5% average probability of an earthquake with $M \geq 7.75$ within five years at an arbitrary location, the segments of the Kuril–Kamchatka arc in which the probability of an event with $M \geq 7.75$ was greater or less than 5% were determined [*Fedotov*, 1974, 2005].

2.4. Formalized Identification of Boundaries for Earthquake Source Areas

During the initial development stages of the method for long-term earthquake prediction, the source area was taken to be an ellipse with an axis ratio of approximately 1/2. Within this ellipse fell about two-thirds of the aftershocks in the first year following an earthquake with $M \geq 7.75$. When delineating the boundaries of the epicentral areas, the mutual positions of the epicenters of strong foreshocks, the mainshock, and aftershock clusters, as well as data on rupture length, the tsunami source, and macroseismic data, were taken into account [*Fedotov*, 2005].

By 1980 [*Fedotov et al.*, 1980], new detailed data on the seismicity in the source areas of earthquakes with $M \geq 7.75$ enabled S. A. Fedotov to introduce formalized rules for determining the boundaries of source areas based on data on their aftershocks and foreshocks [*Fedotov*, 2005]. For that purpose, using a catalog of foreshocks, mainshocks, and aftershocks for the first year for events with $M \geq 7.75$ that occurred during 1958–1979 in the region of the Southern Kuril Islands, isolines of seismic activity A_{10} and of seismic energy release D (based on the first-year aftershocks with $M \geq 6.0$) were constructed [*Fedotov et al.*, 1980]. Various pairs of A_{10} and D isolines were examined, and the conventional median line between the $A_{10} = 10$ and $D = 1$ isolines was adopted as the boundary of the source area. Where such isolines were insufficient to define all source-area boundaries, the boundaries of the area of the first-year aftershocks with $M \geq 6.0$ were additionally employed [*Fedotov*, 2005]. The boundaries thus defined made it possible to substantially refine the source areas of earthquakes with $M \geq 7.75$ and to identify more reliably the probable areas of the next such earthquakes in the Kuril–Kamchatka arc [*Fedotov*, 2005; *Fedotov et al.*, 1980].

The refinement of earthquake source boundaries using the new methodology permitted the division, in the prediction for 1975–1980, of a number of segments into western and eastern parts relative to the Kuril–Kamchatka arc. One such segment was the area adjacent to Avacha Bay, the northwestern part of which, according to the assumptions of S. A. Fedotov, was passing through stage III of the seismic cycle [*Fedotov*, 2005; *Fedotov et al.*, 1980]. In subsequent predictions, the hazard of an earthquake with $M \geq 7.75$ in this segment of the arc remained consistently high [*Fedotov*, 2005; *Fedotov and Chernyshev*, 1983], along with low values of $P(A_{10}) \cdot P(D)$. Note that on the map of D isolines for 1962–1983 [*Fedotov et al.*, 1990], large gradients of seismic energy release were observed in the Avacha Bay area, indicating that, at the end of the 1980s, the Avacha Bay area was one of the most seismically hazardous areas of the Kuril–Kamchatka arc [*Fedotov*, 2005; *Fedotov et al.*, 1990].

2.5. Overall Assessment of the Reliability for the Prediction for 1965–1985

In 1987, an overall assessment of the reliability of the long-term earthquake prediction for 1965–1985 was provided in [*Fedotov and Chernyshev*, 1987]. All five earthquakes with $M \geq 7.75$ (in 1968 with $M = 7.9$ east of the northern part of Honshu Island; in 1969 with $M = 8.2$ off the islands of Kunashir and Iturup; in 1971 with $M = 7.8$ in the Kamchatka Strait between Kamchatka and Bering Island; in 1973 with $M = 7.9$ off Kunashir Island; and in 1978 the swarm of earthquakes with $M = 7.1$–8.0 off Iturup Island [*Fedotov*, 2005]) occurred in the seismic gaps where such earthquakes had been anticipated according to the prediction of S. A. Fedotov [*Fedotov*, 1965, 1984; *Fedotov and Chernyshev*, 2002]. Considering individually the predictions for 1971–1975, 1976–1980, and 1981–1985, it should be noted that the earthquakes with $M \geq 7.75$ were confined to segments with low values of $P(A_{10}) \cdot P(D)$ [*Fedotov*, 2005; *Fedotov and Chernyshev*, 1987].

In the predictions for 1965–1985, the seismic activity A_{10} estimated with a probability of 0.7 was correctly predicted for segments passing through stages I or II of the cycle in 27 out of 37 cases, i.e., 73%. Earthquakes with magnitude $M = 5.75$–6.25, expected with a probability of 0.8 over five-year time intervals, occurred in 24 out of 37 cases, i.e., 65%; earthquakes with $M = 6.25$–7.0, expected with a probability of 0.5, occurred in 12 out of 37 cases, i.e., 32%. At the same time, the prediction of earthquakes with $M = 5.75$–7.0 was successful in 1965–1970 and 1971–1975 and less accurate in 1981–1985 [*Fedotov*, 2005; *Fedotov and Chernyshev*, 1987].

The long-term earthquake prediction for the Kuril–Kamchatka arc by S. A. Fedotov was successful in 1965–1985. Its efficacy was confirmed by a 20-year verification against actual data [*Fedotov*, 2005].

2.6. The “Scenario” of the Foreshock–Aftershock Process

Earthquakes with $M \geq 7.75$ are often preceded by foreshocks and followed by strong aftershocks, which represent a considerable additional hazard. In 1993, in [*Fedotov et al.*, 1994a], S. A. Fedotov studied the average sequence of foreshocks and aftershocks with $M \geq 6.0$ accompanying earthquakes with $M \approx 8.0$. For this purpose, 17 events with $M = 7.8$–8.2 that occurred during 1904–1985 in Kamchatka, the Kuril Islands, Japan, and other parts of the Pacific seismic belt were analyzed, together with their foreshocks and aftershocks with $M \geq 6.0$ that occurred within one month before and after the main event. Note that S. A. Fedotov did not consider earthquakes with $M > 8.2$, treating them as events of a larger, independent class [*Fedotov*, 2005; *Fedotov et al.*, 1994a].

For each of the 17 earthquakes, distributions of the number of foreshocks and aftershocks by magnitude and time (by day over the course of a month and by hour during the first 24 hours) were constructed, as well as cumulative plots of the temporal increase in the average number of events observed in the mainshock source [*Fedotov et al.*, 1994a]. From the results of this construction of a “scenario” for the foreshock–aftershock process, the following should be noted. Within one to two days, and especially in the last 24 hours before an earthquake with $M \approx 8.0$, foreshocks with $M \geq 6.0$ were observed in 27% of cases. The most hazardous are the first 8 hours after the mainshock, during which approximately one-third of all aftershocks of the first month may occur. During the first three days, the hazard of aftershocks with $M \geq 7.5$ is high. After the first week, the probability of events with $M = 7.0$–8.4 decreases substantially. During the first month after the main event, an average of 6–7 aftershocks with $M \geq 6.0$ are observed [*Fedotov*, 2005; *Fedotov et al.*, 1994a].

In 1998, in [*Fedotov et al.*, 1998], the probabilistic “scenario” was extended from one month to one year. For its construction, 12 aftershock sequences that occurred solely within the Kuril–Kamchatka and Japan focal zones were analyzed [*Fedotov*, 2005; *Fedotov et al.*, 1998]. It was shown that 70% of the annual number of aftershocks with $M \geq 6.0$ occur in the first month; in the first 10 days, 92% of the monthly and 65% of the annual number of aftershocks with $M \geq 6.0$, and 97% of the monthly and 95% of the annual number with $M \geq 7.0$. Particular attention was drawn to the first three days, when 75% of the aftershocks with $M \geq 6.0$ over 10 days, 70% over a month, and 50% over a year occur [*Fedotov et al.*, 1998]. Over the course of a month, the process weakens, and in the interval from one month to one year, only single events with $M \geq 6.0$ occur. On average, the strongest aftershock has a magnitude 0.8 units less than the mainshock and occurs 4.4–6.0 days after it. The closer in time the strongest aftershock is to the main event, the weaker it is. In the majority of cases, the strongest aftershock is located at a distance of one-third of the source area length from the mainshock epicenter [*Fedotov*, 2005; *Fedotov et al.*, 1998].

The "scenario" of aftershock sequence development was systematically applied by S. A. Fedotov for predicting seismic hazard after earthquakes with $M \geq 7.7$ [*Fedotov*, 2005]. It is noteworthy that the aftershock sequences with $M \geq 6.0$ of the Shikotan (1994), Kronotsky (1997), Olyutorsky (2006), Middle Kuril (2006), and other earthquakes conformed rather well to this "scenario" [*Fedotov*, 2005; *Fedotov et al.*, 1999, 1994a,b, 2007, 2011]. Note that the prediction estimates for the long-term period of the aftershock process proved to be the most reliable. Despite the fact that the "scenario" was constructed for earthquakes with $M = 7.8$–8.2, the aftershock process of the 2025 megathrust earthquake with $M_W = 8.8$ demonstrates good agreement with it.

2.7. Overall Assessment of the Reliability for the Prediction for 1986–2000

In 2002, S. A. Fedotov carried out an assessment of the reliability of the long-term earthquake prediction for 1986–2000 [*Fedotov and Chernyshev*, 2002]. The source areas of both earthquakes with $M \geq 7.75$ that occurred during this period (the Shikotan earthquake of October 4, 1994 with $M = 8.0$ and the Kronotsky earthquake of December 5, 1997 with $M \geq 7.8$–7.9) were located in the seismic gaps considered to be the most probable areas of the next strongest earthquakes [*Fedotov*, 2005; *Fedotov and Chernyshev*, 2002]. Thus, by 2000, the long-term earthquake prediction for the Kuril–Kamchatka arc had been validated for all 7 earthquakes with $M \geq 7.75$ that occurred during 1965–2000 [*Fedotov*, 2005; *Fedotov and Chernyshev*, 1987, 2002].

Note that during 1965–2000, the application of the parameter $B = P(A_{10}) \cdot P(D)$, that was introduced in [*Fedotov*, 1974], demonstrated high efficacy. For example, beginning in 1971, a monotonic decrease in parameter B was observed in the region of Shikotan Island and the Kronotsky Peninsula. It reached critical values (less than 0.03) prior to the earthquakes. Based on the analysis of parameter B values, a warning that the Shikotan Island area had become, in 1994, the most probable area of the next strong earthquake was sent by S. A. Fedotov to the Ministry of Emergency Situations of Russia five months before the earthquake [*Fedotov and Chernyshev*, 2002; *Fedotov et al.*, 1999]. In the case of the 6 earthquakes (with $M \geq 7.75$ in 1965–2000) for which data were available for 0–5 years prior to them, reduced values of B were observed. In three cases B values less than 0.03 were observed. Moreover, all 6 events occurred in seismic gaps for which, over the preceding 5 years, the lowest values of parameter B had been observed [*Fedotov*, 2005; *Fedotov and Chernyshev*, 2002].

For 1986–2000, the predictions of the $A_{10} \pm \sigma$ values (with a probability of 0.7) and of the magnitude levels (with probabilities of 0.8 and 0.5) remained, on average, at the level of those for 1965–1985 [*Fedotov and Chernyshev*, 1987]. The magnitude level $M(P = 0.8)$ was attained in 57% of cases, and $M(P = 0.5)$ in 30–35% of cases. The A_{10} prediction was confirmed in 53% of cases, which is somewhat lower than in 1965–1985. This is explained by the fact that, after the Shikotan and Kronotsky earthquakes, seismic activity increased substantially not only within their source areas but also in adjacent segments [*Fedotov*, 2005; *Fedotov and Chernyshev*, 2002].

2.8. Development of the Method and the Long-Term Earthquake Prediction for 2001–2005

In 2002, the method of long-term earthquake prediction by S. A. Fedotov underwent further development [*Fedotov and Chernyshev*, 2002]. In constructing the prediction for 2001–2005, in addition to the previously predicted parameters, the probabilities of the occurrence of earthquakes with $M \geq 7.75$ over the next five years were calculated for each identified segment of the Kuril–Kamchatka seismogenic zone (the hazardous seismic gaps in which the last earthquake with $M \geq 7.75$ had occurred before 1920, and the areas where earthquakes with $M \geq 7.75$ had occurred during the preceding 80 years) (Figure 7). For this purpose, such independent data as the regularities of seismic gap distribution, the properties of the seismic cycle and its stages, the duration of the seismic cycle (140 ± 60 years and 120 ± 50 years – the estimate updated by 2000 [*Fedotov*, 2005]), the normal distribution of time intervals between strongest earthquakes at a given location, the average recurrence rate of the strongest earthquakes throughout the Kuril–Kamchatka zone (approximately 5 years), the determination of the relative hazard of seismic gaps, and other data were used [*Fedotov*, 2005; *Fedotov and Chernyshev*, 2002]. Note that the probability estimates thus calculated are proportional to the value $1 - B$ (i.e., they depend on the values of A_{10} and D) and to the length of the arc segment under consideration (Figure 7).

In Figure 7, attention is drawn to the high probability (20.5%) of the occurrence in 2001–2005 of an earthquake with $M \geq 7.75$ in the Avacha Bay area. In turn, the aggregate probability of such an earthquake in Avacha Bay and in the adjacent segment off South Kamchatka (the region containing the source zones of the 1952 and 2025 earthquakes) reaches nearly 40.0%, which constituted half of the probability of an event in all the seismic gaps identified in 2000 [*Fedotov*, 2005; *Fedotov and Chernyshev*, 2002].

2.9. Retrospective Prediction for 2001–2005 for the Hokkaido Island Area

On September 25, 2003, an earthquake with $M_S = 8.1$ occurred off the coast of Hokkaido Island [*Fedotov et al.*, 2004]. Its source did not fall within the zone for which S. A. Fedotov had provided a prediction, being located to the south of it and encompassing the southern part of the 1952 earthquake source (Figure 7) [*Fedotov*, 2005]. In 2004, in [*Fedotov et al.*, 2004], a retrospective prediction for 2001–2005 was constructed for the segment of the Pacific seismic belt located off Hokkaido Island. For this purpose, the beginning of segment 1 was shifted to the southwestern edge of the 1952 earthquake source, up to the line dividing the seismically active zones of Hokkaido and Honshu. A new segment 0 was also added. The estimates of $P(A_{10})$, $P(D)$ and B were obtained under the assumption that the characteristics of the seismic cycle in this area are the same as those for the Kuril–Kamchatka seismofocal zone. This assumption was based on the fact that the region southeast of Hokkaido Island is a continuation of the Kuril–Kamchatka island arc [*Fedotov et al.*, 2004].

The retrospective prediction for 2001–2005 thus constructed showed that the aggregate probability of an earthquake with $M \geq 7.7$ in segments 0 and 1 was 29.6% [*Fedotov*, 2005; *Fedotov et al.*, 2004]. Higher probabilities (38.8% in total) were determined only for South Kamchatka and Avacha Bay (Figure 7). Thus, the seismic gap, encompassing two segments with a total length of 300 km along the southeastern coast of Hokkaido Island, was, in 2001, one of the most hazardous areas within the 2,300-km-long section of the Pacific seismic belt located between the city of Ust-Kamchatsk in Kamchatka and Cape Erimo on Hokkaido [*Fedotov et al.*, 2004].

The retrospective results strongly supported the applicability of the method developed by S. A. Fedotov in new regions. Subsequent mapping of the 2003 earthquake source showed that it covered the most hazardous part of the seismic gap, a large portion of the 1952 earthquake source area ($M = 8.3$), and the western seismic quiescence zone [*Fedotov et al.*, 2004].

2.10. Long-Term Earthquake Prediction for 2004–2011

Long-term earthquake predictions for the Kuril–Kamchatka arc were updated by S. A. Fedotov on a regular basis. New predictions were constructed no less frequently than every six months, or more often if strong earthquakes had occurred and, as a consequence, the seismicity parameters had changed substantially.

In [*Fedotov et al.*, 2004], a prediction was constructed for 2004–2008 (April 2004–March 2009). Its distinctive feature was that, for Kamchatka, the division into prediction segments was performed in two variants. Maps of the prognostic parameter B were also constructed to assess the relative hazard of the seismic gaps. This was done with the aim of refining the prediction for the area of the city of Petropavlovsk-Kamchatsky. The prediction constructed using the classical segmentation scheme showed that the highest probability of an earthquake with $M \geq 7.7$ in 2004–2008 was retained in Avacha Bay (18.9%) and off South Kamchatka (17.1%).

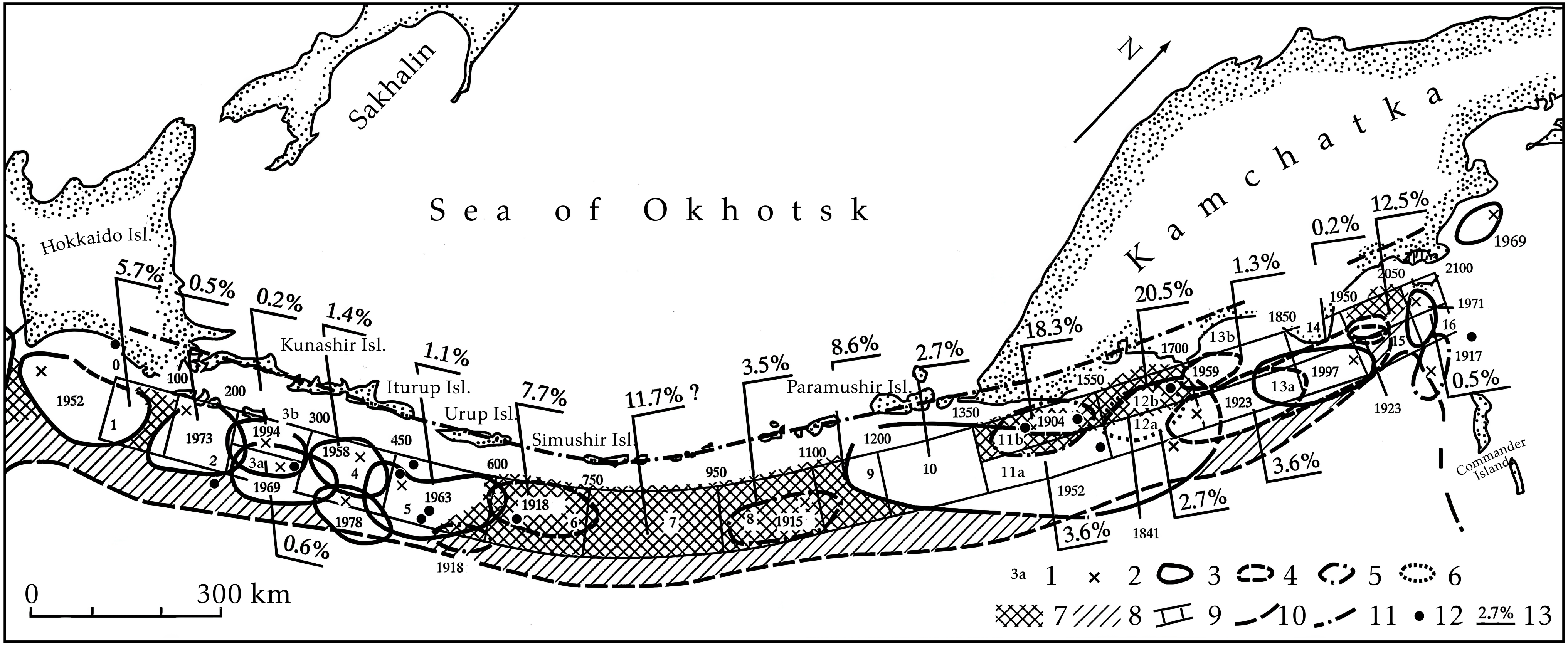

Figure 7. Map of the source areas of the Kuril–Kamchatka earthquakes of 1904–2000 with $M \geq 7.75$, $h = 0$–80 km, and the probabilities of the occurrence of such earthquakes in 2001–2005 in all segments of the prediction strip (from [*Fedotov*, 2005; *Fedotov and Chernyshev*, 2002]): 1 – numbers of the segments for which the long-term earthquake prediction is given; 2 – instrumental epicenters of the mainshocks of earthquakes with $M \geq 7.75$; 3 – boundaries of the source areas of earthquakes with $M \geq 7.75$, drawn with an accuracy of ±10 km; 4 – the same boundaries drawn with lower accuracy; 5 – probable source areas of the 1904–1918 earthquakes with $M \geq 7.75$; 6 – inferred source area of the 1841 earthquake, located in segments 12a and 12b; 7 – most probable areas of the next earthquakes with $M \geq 7.75$; 8 – possible areas of the next earthquakes with $M \geq 7.75$; 9 – boundaries of the prediction strip; 10 – axes of deep-water trenches; 11 – axis of the volcanic belt of the Kuril–Kamchatka arc; 12 – epicenters of the 1991–2000 earthquakes with $M = 7.0$–7.6, $h = 0$–80 km; 13 – probability value (in %) of the occurrence of earthquakes with $M \geq 7.75$ in 2001–2005 in all segments of the Kuril–Kamchatka seismogenic zone for which the long-term earthquake prediction is given.

The increase in the A_{10} and D values at stage III of the seismic cycle may involve not only the source of the approaching earthquake but also the adjacent areas. Proceeding from this, a prediction was constructed in which segments 11a and 11b, 12a and 12b, and 13a and 13b were combined (see, for example, Figure 7). Under the assumption that segment 13 is passing through stage II of the cycle, the following probabilities of the occurrence of an earthquake with $M \geq 7.7$ were obtained for segments 11, 12, and 13: 12.6%, 28.6%, and 3.9%, respectively. In turn, under the assumption of stage III in segment 13, probabilities of 10.3%, 23.4%, and 12.7%, respectively, were obtained.

The mapped isolines of parameter B also indicated that the most probable area for the sources of the next earthquakes with $M \geq 7.7$ was Avacha Bay (segment 12) and the adjacent segments of South Kamchatka (segment 11) and Kronotsky Bay (segment 13). The pattern of the parameter B isolines permitted the assertion that, in Avacha Bay, the outer part farther from the coast is more hazardous [*Fedotov et al.*, 2004].

After [*Fedotov et al.*, 2004], in 2004–2005, S. A. Fedotov updated the predictions several times. They were provided for November 2004–October 2009, June 2005–May 2010, and September 2005–September 2010. The paper [*Fedotov et al.*, 2007] presents the long-term earthquake prediction for the Kuril–Kamchatka arc for April 2006–April 2011. The methodological innovation here was the use of a new parameter, A_{11} – the number of earthquakes of energy class $K_S = 11$ ($M = 4.3$) per year over an area of 1,000 km^2. In turn, $P(A_{11})$ is the probability that A_{11} over most part of the source area of the strongest earthquake, during the 10–15 years preceding it, will be randomly greater than its observed value. Thus, for assessing the relative hazard of seismic gaps, in addition to $B = P(A_{10}) \cdot P(D)$, the parameters $B_1 = P(A_{10}) \cdot P(D) \cdot P(A_{11})$ and $B_2 = P(A_{10}) + P(D) + P(A_{11})$ were also used. The values B_1 and B_2 allow the range of B values to be estimated in the case of low correlation between A_{10}, D and A_{11} and in the case of strong dependence among them [*Fedotov et al.*, 2007].

According to the prediction for April 2006–April 2011, the most probable area of the next earthquake with $M \geq 7.7$ was the Avacha Bay area and the adjacent segments of the island arc, with an aggregate probability of 41.8–48.0%. The second most hazardous area was the region of the Middle Kuril Islands. Here was an increase in the probability of an earthquake with $M \geq 7.7$ from October 2005 to April 2006 from 7.9% to 9.6%. The aggregate probability for this segment together with the adjacent ones was 26.7% [*Fedotov et al.*, 2007].

Eight months after the prediction was made, on November 15, 2006, the Middle Kuril (Simushir) earthquake with $M_S = 8.2$, $M_W = 8.3$ occurred in the region of Simushir Island [*Fedotov et al.*, 2007, 2008]. Its source filled the seismic gap between the sources of the 1915 earthquake with $M = 8.1$ and the 1918 earthquake with $M = 8.3$. The earthquake occurred in full accordance with the predictions provided for 2001–2005, 2004–2008, September 2005–September 2010, and April 2006–April 2011 [*Fedotov et al.*, 2007, 2011]. It is important to note that, in addition to the probable location of the source area, the magnitude of the event was also correctly predicted [*Fedotov et al.*, 2011]. The earthquake became a confirmation of results obtained by S. A. Fedotov indicating the high seismic potential of the segment of the Kuril–Kamchatka arc in the Middle Kuril Islands area. Previously, a number of researchers had considered that earthquakes with $M \geq 7.7$ could not occur there [*Reisner and Rogozhin*, 2003; *Tarakanov et al.*, 1977].

Several weeks after the Middle Kuril (Simushir) earthquake, the long-term earthquake prediction was once again updated (for the period November 2006–October 2011). In its new version, the probability of an earthquake with $M \geq 7.7$ in the Avacha Bay area and the adjacent segments increased to 53%. Following it in terms of seismic hazard level were the areas near the Nemuro Peninsula (11.2%) and Onekotan Island (9.8%), as well as Kamchatka Bay in Kamchatka (9.4%) [*Fedotov et al.*, 2007].

Two months after the Middle Kuril (Simushir) earthquake, a seismic event with $M_S = 8.1$ [*Fedotov et al.*, 2008] occurred in the vicinity of its source, within the oceanic plate in front of the oceanic trench [*Mikhailov et al.*, 2025b]. Note that such a combination of two earthquakes was a rare event, similar to the pair of 1918 with $M = 8.2$ and $M = 7.9$, which also occurred two months apart near the islands of Simushir and Urup.

2.11. Long-Term Earthquake Prediction for 2008–2021

In 2008, using the parameters $A_{10}(t)$ and $D(t)$ refined in [*Fedotov et al.*, 2008], a long-term earthquake prediction was constructed for the period April 2008–March 2013. According to this prediction, the aggregate probability of an earthquake with $M \geq 7.7$ in the segment of the Kuril–Kamchatka arc encompassing South Kamchatka, Avacha Bay, and Kronotsky Bay, which corresponds to shaking intensities of VII–IX in Petropavlovsk-Kamchatsky, was 49.2%. The probability of an earthquake with $M \geq 7.7$ in the Kamchatka Bay area was 8.5%; in the Kuril Islands, in the Onekotan Island–Middle Kuril Islands area, 24.5%; and in the Nemuro Peninsula area, 9.6% [*Fedotov et al.*, 2008].

In turn, in the predictions for the periods September 2010–August 2015 [*Fedotov et al.*, 2011] and September 2011–August 2016 [*Fedotov et al.*, 2012], the probability of an earthquake with $M \geq 7.7$ in the Avacha Bay area and the adjacent segments of the Kuril–Kamchatka arc was 54.0% and 52.2%, respectively. The aggregate seismic hazard in the Middle Kuril Islands area (the seismic gaps south and north of the source of the Middle Kuril (Simushir) earthquake) was 23.8% [*Fedotov et al.*, 2011] and 24.6% [*Fedotov et al.*, 2012]; in the Kamchatka Bay area, 6.9% [*Fedotov et al.*, 2011] and 7.5% [*Fedotov et al.*, 2012]; and in the Nemuro Peninsula area, 6.5% [*Fedotov et al.*, 2011] and 6.6% [*Fedotov et al.*, 2012].

The study of the total released seismic energy, both in the entire Kuril–Kamchatka region and in its individual parts, was employed by S. A. Fedotov as an important supplement to the method of long-term earthquake prediction [*Fedotov et al.*, 2012]. *Fedotov et al.* [2011] analyzed data on the accumulation and release of seismic energy in the Kuril–Kamchatka seismogenic zone from 1900 to 2010. It was shown that, since 1952, seismic energy equivalent to an earthquake with $M = 8.5$ had been accumulated in the Kamchatka area [*Fedotov and Solomatin*, 2015]. If an earthquake of such magnitude were to occur, it would most likely encompass the entire seismic gap in South Kamchatka and Avacha Bay. The probable time of such an earthquake was estimated as the end of 2011 ± 1 year, with the latest possible date being 2015–2023 [*Fedotov et al.*, 2011].

In 2012, the analysis of the similar development of the foreshock, mainshock, and aftershock sequences of the Ozernovsky (November 22, 1969, $M = 7.7$), Ust-Kamchatsky (December 15, 1971, $M = 7.8$), and Kronotsky (December 5, 1997, $M = 7.8$–7.9) earthquakes allowed S. A. Fedotov to draw the following important conclusions [*Fedotov et al.*, 2012]. Seismic processes in Kamchatka had developed in such a way that the sources of earthquakes with $M \geq 7.7$ migrated from north to south, successively filling the seismic gaps. In this process, foreshock chains and swarms originated in the northern part of the earthquake source areas. The main events occurred within the foreshock swarms or to the south of them. Strong aftershock swarms propagated hundreds of kilometers southward from the mainshock epicenter. Based on the revealed regularities in the migration of seismicity, it was hypothesized that the rupture initiation and foreshocks of the next Kamchatka earthquake with $M \geq 7.7$ would be located in the Shipunsky Peninsula region, and its source area would fill the seismic gaps in Avacha Bay and off the coast of South Kamchatka [*Fedotov et al.*, 2012].

In [*Fedotov et al.*, 2012] it is noted that, in 2005, a tentative long-term earthquake prediction had been constructed for northeastern Japan for the period 2005–2010. Within its framework, a large seismic gap was identified off the eastern coast of Japan. Based on the seismic history of this area and the seismic cycle duration of 140 ± 60 years, it had been regarded since the 1980s as the probable area of future earthquakes with $M \geq 7.7$. This seismic gap was filled in 2011 by the source of the catastrophic Tohoku earthquake with $M \geq 9.0$ [*Ozawa et al.*, 2011; *Simons et al.*, 2011]. This provided a further argument both in favor of the applicability of the method of long-term earthquake prediction developed by S. A. Fedotov in general and for the territory of Japan in particular.

In [*Fedotov and Solomatin*, 2015, 2017], S. A. Fedotov presented predictions for the periods September 2013–August 2018 and April 2016–March 2021, respectively. The most probable areas of the next earthquakes with $M \geq 7.7$ remained the segments located in the area of Petropavlovsk-Kamchatsky and South Kamchatka, with an aggregate probability of 42.0% [*Fedotov and Solomatin*, 2015] and 43.7% [*Fedotov and Solomatin*, 2017]. A high level of seismic hazard was observed in the Kamchatka Bay area – 6.8% [*Fedotov and Solomatin*, 2015] and 8.9% [*Fedotov and Solomatin*, 2017]. In the Kuril Islands, the highest seismic hazard level was in the Middle Kuril Islands area – 34.5% [*Fedotov and Solomatin*, 2015] and 29.7% [*Fedotov and Solomatin*, 2017]. The segment near the Nemuro Peninsula had probabilities of 7.1% [*Fedotov and Solomatin*, 2015] and 7.1% [*Fedotov and Solomatin*, 2017].

2.12. The Influence of a Series of Deep Earthquakes on the Development of the Seismic Process in the Kuril–Kamchatka Region

In 2015–2019, S. A. Fedotov analyzed the influence of a series of deep earthquakes beneath the Sea of Okhotsk (July 5, 2008, $M_W = 7.7$; August 14, 2012, $M_W = 7.7$; and the Sea of Okhotsk earthquake of May 24, 2013, $M_W = 8.3$), the Tohoku megathrust earthquake (March 11, 2011, $M_W = 9.0$), as well as the Near-Aleutian earthquake (July 17, 2017, $M = 7.7$), on the development of the seismic process in the Kuril–Kamchatka region [*Fedotov and Solomatin*, 2015, 2017, 2019]. In particular, high values of the A_{10} parameter, constructed for the period 2008–2016, were identified at the northeastern and southwestern boundaries of the source area of the 1952 Kamchatka earthquake with $M = 8.5$ [*Fedotov and Solomatin*, 2017]. The area of maximum A_{10} values was located along the extension of the line "epicenter of the Sea of Okhotsk earthquake – Avacha Bay". This maximum was largely determined by the seismic activation of May 18–24, 2013, which occurred here immediately prior to the Sea of Okhotsk earthquake.

It was noted that the identified areas of high A_{10} values delineate the projection of the deep source of the Sea of Okhotsk earthquake onto the shallow-earthquake region adjacent to the deep-water trench. They are situated at the edges of the seismic gap, which extends 500 km from the Shipunsky Peninsula through Avacha Bay and South Kamchatka to the area of Paramushir Island. This fact, together with the precise temporal coincidence of the activation in Avacha Bay with the deep Sea of Okhotsk earthquake, indicated the existence of a connection between the seismogeodynamic processes in the deep and upper parts of the seismogenic zone and revealed the location of the most highly stressed segments of the upper part of the Kuril–Kamchatka seismogenic zone. Based on the revealed relationships, S. A. Fedotov concluded that the next destructive earthquake should be expected within the seismic gap in South Kamchatka. The seismic energy accumulated there corresponds to an earthquake of magnitude $M = 8.0–9.0$ [*Fedotov and Solomatin*, 2017].

2.13. Long-Term Earthquake Prediction for 2019–2024

The paper [*Fedotov and Solomatin*, 2019] was published at the end of 2019. This is the last article by S. A. Fedotov on the long-term earthquake prediction for the Kuril–Kamchatka arc, which appeared after his death. It provided a prediction for the period June 2019–May 2024 (Figure 8). According to this prediction, the most probable areas of the next earthquakes with $M \geq 7.7$ during the specified five-year period remained the segments located in the Avacha Bay and South Kamchatka. The aggregate probability of earthquakes in those segments (11a, 11b, 12a, 12b, 13a, and 13b in Figure 8) capable of producing shaking intensities of VII–IX in Petropavlovsk-Kamchatsky was 47.6%. Specifically, the probability of an event with an intensity of IX (segment 12b in Figure 8) was 14.2%, while the probability for events with intensities of VIII and VII (segments 11a, 11b, 12a, 13a, and 13b in Figure 8) was 33.4%. It was noted that the probability of the earthquake with an intensity of IX in Petropavlovsk-Kamchatsky during this period was four times higher than the average long-term hazard for the Kuril–Kamchatka seismogenic zone.

In the Kuril Islands, the highest seismic hazard was in the region of the Middle Kuril Islands (segments 6, 8, and 9 in Figure 8), near the ends of the main rupture of the Middle Kuril (Simushir) earthquake. The probability of an earthquake with $M \geq 7.7$ in these seismic gaps was estimated as 6.9%, 9.4%, and 9.7%, respectively [*Fedotov and Solomatin*, 2019].

For the period June 2019–May 2024, a high seismic hazard remained in the area of Kamchatka Bay (segment 15 in Figure 8), with probability of the strongest earthquake of 8.4%. In turn, the analogous probability in the Nemuro Peninsula area was 6.2%. In the remaining segments of the Kuril–Kamchatka seismogenic zone, the probability of an earthquake with $M \geq 7.7$ was either equal to the average or considerably, up to 10 times, lower than the average five-year probability of 3.6–4.2% [*Fedotov and Solomatin*, 2019].

S. A. Fedotov noted that during the five-year period preceding the prediction [*Fedotov and Solomatin*, 2019], an increase in seismic activity of varying degrees had been observed precisely in the identified seismic gaps, primarily in segments 1, 11b, 12b, and 13a (Figure 8). At the same time, segment 10 in the Northern Kurils that is located between two of the largest seismic gaps, was characterized by high seismic activity, indicating the possibility that it could be involved into the source area of the next strongest earthquake.

2.14. Kamchatka Megathrust Earthquake of July 29, 2025

As noted in the introduction, on July 29, 2025 a megathrust earthquake with $M_W = 8.8$ occurred in the Avacha Bay area. A detailed description of this event is provided in [*Chebrov*, 2025; *Chebrov et al.*, 2026]. The present section examines this event in terms of its consistency with the results of semicentennial research by S. A. Fedotov on the long-term earthquake prediction for the Kuril–Kamchatka arc.

Figure 8 demonstrates that the source zone of the 2025 megathrust earthquake [*Chebrov*, 2025] encompassed segments 10, 11a, 11b, 12a, 12b, 13a, and 13b of the Kuril–Kamchatka arc. According to S. A. Fedotov's posthumously published 2019 prediction for June 2019–May 2024, the aggregate probability of the strongest earthquake occurring within these segments was 50.4% [*Fedotov and Solomatin*, 2019]. Comparing the 2025 source area with this prediction is justified, as it shows negligible differences from the 2020–2028 predictions developed in 2021–2024 by successors of S. A. Fedotov [*Solomatin*, 2021, 2022, 2024; *Solomatin and Soldatov*, 2023].

In particular, according to those predictions, the probability of the strongest event within the zone covered by the 2025 earthquake source ranged from 48.6 to 49.4%.

The consistency between the location of the 2025 megathrust earthquake source and the long-term assessments of S. A. Fedotov should be noted. As early as 1980, in [*Fedotov et al.*, 1980] the Avacha Bay area was identified as one of the segments of the Kuril–Kamchatka arc where the next strongest earthquakes were to be expected. Subsequently, in 1987, the establishment of large gradients of seismic energy release in this region, reported in [*Fedotov et al.*, 1990], confirmed the high seismic hazard of this segment.

It is important to note that since 2002, the probabilities of the occurrence for the strongest earthquake over the subsequent five-year interval began to be calculated for each segment of the Kuril–Kamchatka seismogenic zone [*Fedotov and Chernyshev*, 2002]. Since then, the segments in southern Kamchatka and the Avacha Bay area have been consistently identified as the most probable area of the next catastrophic earthquake. Over the course of two decades, the cumulative probability of the strongest earthquake within the segments later covered by the 2025 earthquake source remained steadily at 45–50% and above.

In 2015, S. A. Fedotov demonstrated that the seismic energy accumulated after the 1952 North Kuril earthquake could be released in the near future as an event with $M = 8.5$. The source area of this event would fill the seismic gaps in South Kamchatka and Avacha Bay [*Fedotov and Solomatin*, 2015]. In 2017, it was noted that the next strongest earthquake with $M = 8.0$–9.0 would occur precisely within these seismic gaps [*Fedotov and Solomatin*, 2017]. At the same time, despite the low individual probability of an event with $M \geq 7.7$ for segment 10 (Figure 8), its level of seismic activity indicated the potential for this segment to be involved to the source area of the next strongest earthquake in South Kamchatka [*Fedotov and Solomatin*, 2019].

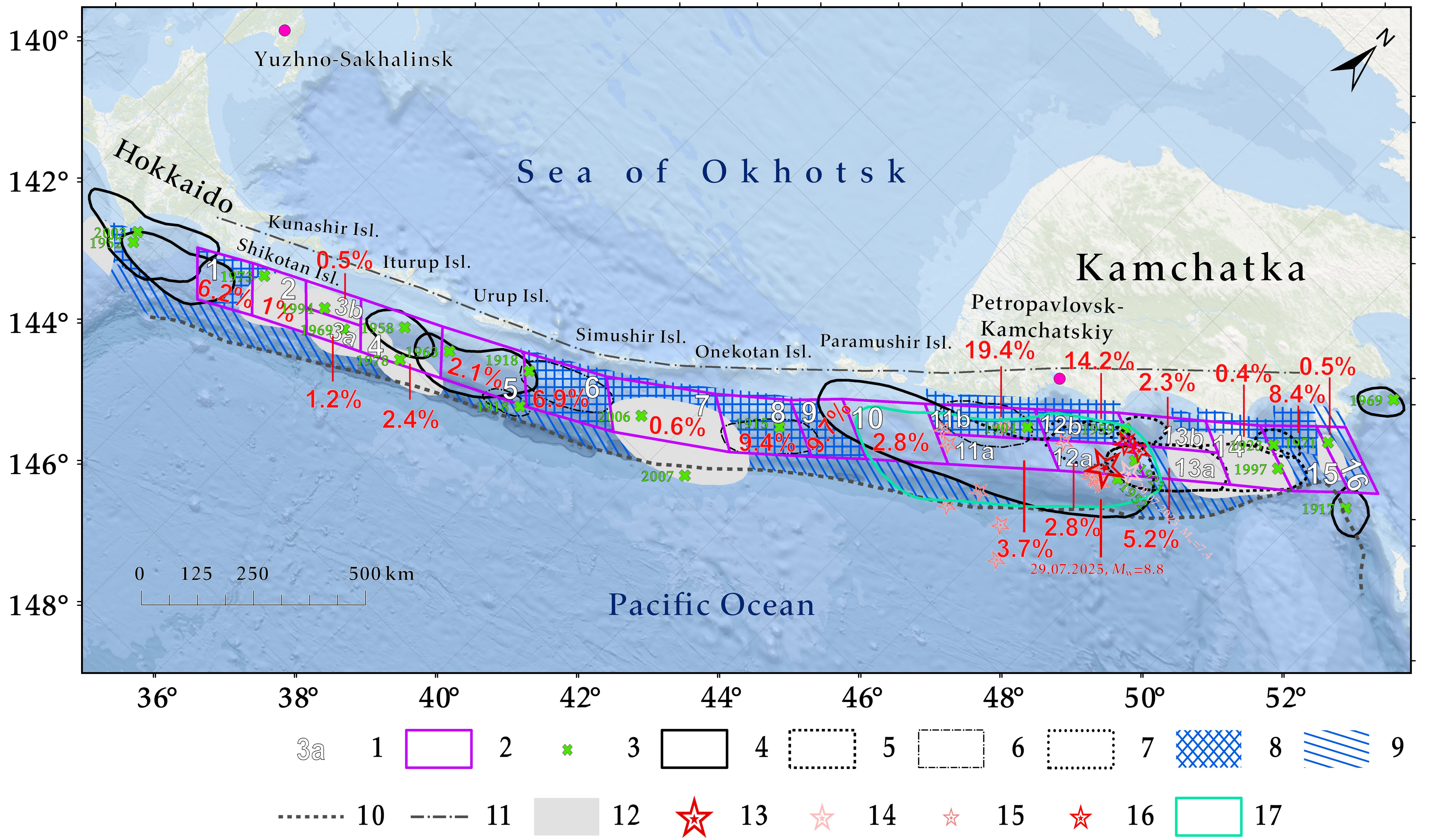

Figure 8. Caption on next page.

Figure 8. Long-term earthquake prediction for the Kuril–Kamchatka arc, source areas of the Kuril–Kamchatka earthquakes of 1902–2019 with $M \geq 7.7$, probabilities of the occurrence of shallow ($H < 80$ km) earthquakes with $M \geq 7.7$ in the period June 2019–May 2024 (according to [*Fedotov and Solomatin*, 2019]), and the epicenter of the Kamchatka megathrust earthquake of July 29, 2025 with $M_W = 8.8$: 1 – numbers of the segments for which the long-term earthquake prediction is given; 2 – boundaries of the prediction segments; 3 – instrumental epicenters of the mainshocks of earthquakes with $M \geq 7.7$; 4 – boundaries of earthquake source areas with $M \geq 7.7$, drawn with an accuracy of ±10 km; 5 – segments of the same boundaries drawn with lower accuracy; 6 – probable source areas of the 1904–1918 earthquakes with $M \geq 7.7$; 7 – inferred source area of the 1841 earthquake; 8 – most probable areas of the next earthquakes with $M \geq 7.7$; 9 – possible areas of the next earthquakes with $M \geq 7.7$; 10 – axes of deep-water trenches; 11 – axis of the volcanic belt of the Kuril–Kamchatka arc; 12 – source areas of earthquakes with $M \geq 7.7$ that occurred after 1965 in the predicted seismic gaps; 13 – epicenter of the Kamchatka megathrust earthquake of July 29, 2025 with $M_W = 8.8$; 14 – epicenter of the Kamchatka earthquake of July 20, 2025 with $M_W = 7.4$; 15 – epicenters of aftershocks of the Kamchatka megathrust earthquake with $M_W \geq 6.0$; 16 – epicenters of the strongest aftershocks of the Kamchatka megathrust earthquake with $M_W = 7.4$ and $M_W = 7.8$; 17 – source area of the Kamchatka megathrust earthquake of July 29, 2025 with $M_W = 8.8$ (according to [*Chebrov*, 2025]).

The hypothesis advanced in 2012 in [*Fedotov et al.*, 2012] that the rupture initiation and a foreshock of the next strongest earthquake would be localized in the area of the Shipunsky Peninsula, and that the aftershock cloud would extend hundreds of kilometers southward from the mainshock epicenter, was fully corroborated by the actual development of the seismic process within the source of the 2025 event. The spatial configuration of the source similarly confirmed conclusion made by S. A. Fedotov that, in Avacha Bay, the greatest hazard is posed by its outer part, which is farther from the coast [*Fedotov et al.*, 2004].

The foregoing indicates that the location, magnitude, and character of the source process of the 2025 $M_W = 8.8$ megathrust earthquake are in complete agreement with the results of S. A. Fedotov. The actual occurrence of the event within the seismic gaps of South Kamchatka and Avacha Bay, which for decades had been characterized as the probable area of the next strongest earthquake, constitutes empirical proof of the high efficacy and fundamental validity of the methodology of long-term earthquake prediction for the Kuril–Kamchatka arc developed by Sergey A. Fedotov.

Note that, despite the substantial spatial overlap of the source zones of the 2025 and 1952 events (Figure 8) [*Chebrov*, 2025], the interval between the two megathrust earthquakes amounted to 73 years. This interval lies below the threshold value of the seismic cycle duration originally estimated by S. A. Fedotov in 1968 as 140 ± 60 years [*Fedotov*, 1968]. However, it falls within the limits of the cycle refined in 2002 to 120 ± 50 years [*Fedotov and Chernyshev*, 2002].

In [*Mikhailov et al.*, 2025a] it is suggested that the relatively short interval between the megathrust earthquakes may be a consequence of the fact that their source areas do not coincide but complement each other. That is, in 1952 and 2025 the main slip may have occurred on different segments of the subduction zone: on segments located closer to and farther from the deep-water trench. In other words, during the inter-event period stress accumulated not uniformly across the entire zone but concentrated in those segments that did not release strain during the preceding megathrust earthquake. It is worth noting that in [*Fedotov*, 1968], S. A. Fedotov formulated the hypothesis that a part of the arc segment in the Avacha Bay area could have lain outside the source area of the 1952 megathrust event. It is possible that the preceding megathrust earthquake for this segment should be considered the event of 1841 (see the source area boundaries in Figure 2).

According to [*Lobkovsky et al.*, 2026], the interval between Kamchatka megathrust earthquakes may be governed by the fact that, within the framework of the key–block model [*Lobkovsky et al.*, 1991], the South Kamchatka segment of the frontal wedge is monolithic (highly consolidated). It lacks large longitudinal faults that could partially release the accumulated stress. That is, if the wedge is not fragmented, elastic strain energy accumulates almost synchronously over the entire plate interface, and the critical Coulomb stress is reached relatively rapidly.

3. Conclusion

The long-term earthquake prediction method developed in the mid-1960s by Sergey A. Fedotov [*Fedotov*, 1967] is based on the concept of seismic gaps [*Fedotov*, 2005], and represents a fundamental contribution to seismology in the second half of the 20th century. Within this approach, the concept of the seismic cycle was first formulated [*Fedotov*, 1968] and a quantitative estimate of its duration for the Kuril–Kamchatka Arc was given [*Fedotov*, 2005].

As noted in [*McCann et al.*, 1979], the method developed by S. A. Fedotov was a significant breakthrough in seismology as it was proposed at the initial stages of the development of plate tectonics theory. This approach made it possible to move from a predominantly statistical description of seismicity in subduction zones to physically based quantitative estimates of seismic hazard. The results of research by S. A. Fedotov were regularly discussed by the international expert community and were considered a model of system analysis of long-term seismic hazard.

The research of S. A. Fedotov was predominantly focused on the Kuril–Kamchatka region. At the same time, the developed method was also applied in other regions of the Pacific seismic ring – from the Aleutian arc to the coast of Chile. The results obtained by S. A. Fedotov initiated numerous studies based on the concept of seismic gaps and are actively developed by leading scientific teams to this day [*Kanamori et al.*, 1993; *Kelleher*, 1972; *McCann et al.*, 1979; *Mogi*, 1969; *Perez and Jacob*, 1980; *Plata-Martinez et al.*, 2021; *Sykes*, 1971].

Analysis of the long-term earthquake predictions made by S. A. Fedotov demonstrates a high level of their reliability. For example, within the studied Kuril–Kamchatka Arc, since 1965, the sources of all earthquakes with $M \geq 7.75$ were located within the seismic gaps identified as the most probable locations for the next strongest earthquakes in given five-year periods. These events include:

- 1968, with $M = 7.9$ east of the northern part of Honshu Island;
- 1969, with $M = 8.2$ off the islands of Kunashir and Iturup;
- 1971, with $M = 7.8$ in the Kamchatka Strait between Kamchatka and Bering Island;
- 1973, with $M = 7.9$ off Kunashir Island;
- 1978, a swarm of earthquakes with $M = 7.1$–8.0 off Iturup Island;
- 1997, Shikotan earthquake with $M = 8.0$;
- 1997, Kronotsky earthquake with $M \geq 7.8$–7.9;
- 2003, earthquake off Hokkaido with $M_S = 8.1$ (retrospective prediction);
- 2006, Central Kuril (Simushir) earthquake with $M_W = 8.3$;
- 2011, Tohoku earthquake with $M = 9.0$;
- 2025, Kamchatka megathrust earthquake with $M_W = 8.8$.

It is important to note that, in addition to the source areas, the magnitudes of the events were also very successfully predicted.

The most important applied result of half-century research by S. A. Fedotov is the prediction of the location and magnitude of the megathrust earthquake that occurred on July 29, 2025, in Southern Kamchatka. This event became one of the strongest instrumentally recorded in the Pacific Ocean – Okhotsk Plate transition zone and the first in the 21st century to confirm the long-term earthquake prediction by S. A. Fedotov on such a large scale.

The results of the long-term earthquake prediction formed the basis for strategic planning of seismic safety measures in the Russian Far East, particularly in the territory of Petropavlovsk-Kamchatsky. The initiatives of S. A. Fedotov, supported by the USSR

Academy of Sciences and the Russian Academy of Sciences, the governments of the USSR and the Russian Federation, and the administration of Kamchatka Krai, became the scientific basis for a set of measures to seismically reinforce buildings and structures. On this basis, orders and resolutions of the Council of Ministers of the USSR (1986 and 1989), the Council of Ministers of the RSFSR (1987), the Government of the Russian Federation (1995 and 2001), and a number of state decisions (2002–2016) on preparing Kamchatka Krai for strong earthquakes were adopted. In 2009, the Government of the Russian Federation approved the federal target program “Increasing the stability of residential buildings, main facilities and life support systems in seismic regions of the Russian Federation for 2009–2018”. In 2013, the Government of Kamchatka Krai approved the target program “Increasing the stability of residential buildings, main facilities and life support systems in Kamchatka Krai for 2013–2015” [*Fedotov*, 2005; *Fedotov and Solomatin*, 2015, 2017, 2019]. By 2017, 75% of residential buildings in Petropavlovsk-Kamchatsky had received the necessary seismic reinforcement [*Fedotov and Solomatin*, 2017].

Advance scientifically based knowledge of the seismic hazard level provided the opportunity for targeted strengthening of buildings, improvement of warning and evacuation algorithms. As a result, in 2025, human casualties and massive destruction were avoided. Thus, the method developed by S. A. Fedotov confirmed its effectiveness not only as a theoretical concept but also as a fundamental basis for state policy on seismic risk management.

The presented review of scientific papers by S. A. Fedotov allows the conclusion that the long-term earthquake prediction method that was developed for the Kuril–Kamchatka Arc is a fundamental stage in the development of Earth sciences and a striking example of a consistent transition from empirical observations to a formalized, physically based prediction system. The quantitative parameters included in the method, describing the dynamics of the seismic process in the subduction zone, ensure its relevance in the modern period.

The long-term earthquake prediction method by S. A. Fedotov has been successfully verified by an event of planetary scale. The 2025 Kamchatka megathrust earthquake not only did not refute but convincingly confirmed its main provisions.

The list of references of this article consists of more than 100 publications and is of independent interest. This extensive bibliography can serve as a basis for continuing and developing further research on long-term seismic hazard assessment.

Acknowledgments. This work was carried out in the framework of budgetary funding of the Geophysical Center of the Russian Academy of Sciences and the Schmidt Institute of Physics of the Earth of the Russian Academy of Sciences, adopted by the Ministry of Science and Higher Education of the Russian Federation. The authors thank D. D. Veis, Junior Research Scientist of the Geophysical Center of the Russian Academy of Sciences, for assistance in preparing illustrative material in GIS.

References

Beck S. and Christensen D. Rupture process of the February 4, 1965, Rat Islands Earthquake // Journal of Geophysical Research: Solid Earth. — 1991. — Vol. 96, B2. — P. 2205–2221. — https://doi.org/10.1029/90jb02092

Beck S. L. and Ruff L. J. Rupture process of the Great 1963 Kurile Islands Earthquake Sequence: Asperity interaction and multiple event rupture // Journal of Geophysical Research: Solid Earth. — 1987. — Vol. 92, B13. — P. 14123–14138. — https://doi.org/10.1029/jb092ib13p14123

Bilek S. L. and Lay T. Subduction zone megathrust earthquakes // Geosphere. — 2018. — Vol. 14, no. 4. — P. 1468–1500. — https://doi.org/10.1130/ges01608.1

Chebrov D. V. The Mw = 8.8 Kamchatka Megathrust Earthquake of July 29, 2025 // Bulletin of KRAESC. Earth Sciences. — 2025. — 3(67). — P. 113–117. — https://doi.org/10.31431/1816-5524-2025-3-67-113-117 — (In Russian).

Chebrov D. V., Matveenko E. A., Abubakirov I. R., et al. The July 29, 2025 Kamchatka Earthquake, MW 8.9: Examination Based on Regional Data Through End-2025 // Russian Journal of Earth Sciences. — 2026. — Vol. 26. — ES2006. — https://doi.org/10.2205/2026es001116

Cifuentes I. The 1960 Chilean Earthquakes // Journal of Geophysical Research: Solid Earth. — 1989. — Vol. 94, B1. — P. 665–680. — https://doi.org/10.1029/jb094ib01p00665

Delouis B., Nocquet J.-M. and Vallée M. Slip distribution of the February 27, 2010 Mw = 8.8 Maule Earthquake, central Chile, from static and high-rate GPS, InSAR, and broadband teleseismic data // Geophysical Research Letters. — 2010. — Vol. 37, no. 17. — https://doi.org/10.1029/2010gl043899

DeMets C., Gordon R. G. and Argus D. F. Geologically current plate motions // Geophysical Journal International. — 2010. — Vol. 181, no. 1. — P. 1–80. — https://doi.org/10.1111/j.1365-246x.2009.04491.x

Di Giacomo D., Engdahl E. R. and Storchak D. A. The ISC-GEM Earthquake Catalogue (1904-2014): status after the Extension Project // Earth System Science Data. — 2018. — Vol. 10, no. 4. — P. 1877–1899. — https://doi.org/10.5194/essd-10-1877-2018

Dzeboev B. A., Agayan S. M., Zharkikh Yu. I., et al. Strongest Earthquake-Prone Areas in Kamchatka // Izvestiya, Physics of the Solid Earth. — 2018a. — Vol. 54, no. 2. — P. 284–291. — https://doi.org/10.1134/s1069351318020052

Dzeboev B. A., Gvishiani A. D., Agayan S. M., et al. System-Analytical Method of Earthquake-Prone Areas Recognition // Applied Sciences. — 2021. — Vol. 11, no. 17. — P. 7972. — https://doi.org/10.3390/app11177972

Dzeboev B. A., Krasnoperov R. I., Belov I. O., et al. Modified algorithmic system FCAZm and strong earthquake-prone areas in California // Geoinformatika. — 2018b. — No. 2. — P. 2–8. — (In Russian).

Fedotov S. A. Determination of the tsunami source areas during the Kamchatka earthquake of 4 November 1952 and the Iturup earthquake of 6 November 1958 // Izvestiya AN SSSR. Seriya Geofizicheskaya. — 1962. — No. 10. — P. 1333–1339. — (In Russian).

Fedotov S. A. On Patterns Observed in the Locations of Large Earthquakes in Kamchatka, the Kuril Islands, and Northeastern Japan // Trudy IFZ AN SSSR. — 1965. — No. 36. — P. 66–93. — (In Russian).

Fedotov S. A. Long-term seismic forecast for the Kuril-Kamchatka region // The Tsunami Problem. — Moscow : Nauka, 1967. — P. 121–132. — (In Russian).

Fedotov S. A. On the Seismic Cycle, Possibilities of Quantitative Seismic Zonation, and Long-term Earthquake Prediction // Seismic Zonation of the USSR. — Moscow : Nauka, 1968. — P. 121–150. — (In Russian).

Fedotov S. A. On the seismicity of the source area of the catastrophic Iturup earthquake of 6.XI 1958 and the seismic forecast // Izvestiya AN SSSR. Fizika Zemli. — 1969. — No. 1. — P. 3–12. — (In Russian).

Fedotov S. A. The Energy Classification of Earthquakes and the Magnitude Problem. — Moscow : Nauka, 1972. — 116 p. — (In Russian).

Fedotov S. A. Realization of the long-term seismic forecast for the Pacific focal zone off the Kuril-Kamchatka arc for 1965-1970 and a refined forecast for 1971-1975 // Seismicity and Seismic Forecast, Upper Mantle Properties and Their Relation to Volcanism in Kamchatka. — Novosibirsk : Nauka, 1974. — P. 101–109. — (In Russian).

Fedotov S. A. On the development of research on the prediction of earthquakes, tsunamis and volcanic eruptions in the Far East // Vestnik Akademii Nauk SSSR. — 1984. — No. 2. — P. 2–3. — (In Russian).

Fedotov S. A. A Review of Twenty-Five Years of Detailed Seismic Studies of Kamchatka and Commander Islands, November 1961-October 1986: History, Development and Tasks // Vulcanologiya i Sejsmologiya. — 1987. — No. 6. — P. 3–10. — (In Russian).

Fedotov S. A. Long-Term Seismic Forecast for the Kuril-Kamchatka Arc. — Moscow : Nauka, 2005. — 303 p. — (In Russian).

Fedotov S. A. Fifty years of detailed seismological investigations: The Kuril-Kamchatka arc // Journal of Volcanology and Seismology. — 2008. — Vol. 2, no. 2. — P. 135–141. — https://doi.org/10.1134/s0742046308020061

Fedotov S. A. Fifty years of research at the Institute of Volcanology, Siberian Branch, USSR Academy of Sciences - Institute of Volcanology and Seismology, Far East Branch, Russian Academy of Sciences, 1962-2012: its prehistory, activities, and achievements // Vulcanologiya i Sejsmologiya. — 2013. — No. 2. — P. 3–11. — https://doi.org/10.7868/S020303061302003X — (In Russian).

Fedotov S. A., Bagdasarova A. M., Kuzin I. P., et al. Earthquakes and the deep structure of the southern Kuril island arc. — Moscow : Nauka, 1969. — 212 p. — (In Russian).

Fedotov S. A. and Chernyshev S. D. Realization of the long-term seismic prediction for the Kuril-Kamchatka arc for 1976-1980 and prediction for 1981-1985 // Vulcanologiya i Sejsmologiya. — 1983. — No. 5. — P. 74–80. — (In Russian).

Fedotov S. A. and Chernyshev S. D. Twenty Years of Long-term Earthquake Prediction for the Kuril-Kamchatka Arc: the Reliability in 1981-1985, in 1965-1985 Overall, and the Forecast for 1986-1990 // Vulcanologiya i Sejsmologiya. — 1987. — No. 6. — P. 93–109. — (In Russian).

Fedotov S. A. and Chernyshev S. D. Long-term Earthquake Prediction for the Kuril-Kamchatka Arc: Reliability in 1986-2000, the Development of the Method, and the Forecast for 2001-2005 // Vulcanologiya i Sejsmologiya. — 2002. — No. 6. — P. 3–24. — (In Russian).

Fedotov S. A., Chernyshev S. D., Chernysheva G. V., et al. Refining the boundaries of the M ≥ 7 3/4 earthquake rupture areas, the properties of the seismic cycle, and the long-term earthquake forecast for the Kuril-Kamchatka arc // Vulcanologiya i Sejsmologiya. — 1980. — No. 6. — P. 52–67. — (In Russian).

Fedotov S. A., Chernyshev S. D., Matvienko Yu. D., et al. The Forecast of the December 5, 1997, Magnitude 7.8-7.9 Kronotsky Earthquake, Kamchatka, and Its M ≥ 6 Aftershocks // Volcanology & Seismology. — 1999. — Vol. 20, no. 6. — P. 597–613.

Fedotov S. A., Chernysheva G. V. and Shumilina L. S. Earthquake Hazard Due to M > 6 Events that Accompany Great (M = 8) Pacific Earthquakes // Volcanology & Seismology. — 1994a. — Vol. 15, no. 6. — P. 637–648.

Fedotov S. A., Dolbilkina N. A., Morozov V. N., et al. Investigation on Earthquake Prediction in Kamchatka // Tectonophysics. — 1970. — Vol. 9, no. 2/3. — P. 249–258. — https://doi.org/10.1016/0040-1951(70)90020-x

Fedotov S. A., Gusev A. A. and Boldyrev S. A. Progress of Earthquake Prediction in Kamchatka // Tectonophysics. — 1972. — Vol. 14, no. 3/4. — P. 279–286. — https://doi.org/10.1016/0040-1951(72)90076-5

Fedotov S. A., Potapova O. V., Chernysheva G. V., et al. Earthquake hazard from M ≥ 6 aftershocks of great (M > 7.7) earthquakes in the Kuril-Kamchatka and Japan Island Arcs // Volcanology & Seismology. — 1998. — Vol. 20, no. 1. — P. 93–109.

Fedotov S. A., Shumilina L. S. and Chernysheva G. V. The Seismicity of Kamchatka and the Commander Islands as Revealed by Detailed Studies // Volcanology & Seismology. — 1990. — Vol. 9, no. 6. — P. 861–906.

Fedotov S. A., Shumilina L. S., Chernysheva G. V., et al. The Long-term Forecast/Prediction and the Source Evolution of the October 4, 1994 Shikotan Earthquake // Federal'naya sluzhba seismologicheskikh nablyudenii i prognoza zemletryasenii. Informatsionno-analiticheskii byulleten'. Ekstrennyi vypusk. — 1994b. — P. 56–67. — (In Russian).

Fedotov S. A., Sobolev G. A., Boldyrev S. A., et al. Long- and Short-Term Earthquake Prediction in Kamchatka // Tectonophysics. — 1977. — Vol. 37, no. 4. — P. 305–321. — https://doi.org/10.1016/0040-1951(77)90054-3

Fedotov S. A. and Solomatin A. V. The long-term earthquake forecast for the Kuril-Kamchatka island arc for the September 2013 to August 2018 period; the seismicity of the arc during preceding deep-focus earthquakes in the sea of Okhotsk (in 2008, 2012, and 2013 at M = 7.7, 7.7, and 8.3) // Journal of Volcanology and Seismology. — 2015. — Vol. 9, no. 2. — P. 65–80. — https://doi.org/10.1134/S0742046315020025

Fedotov S. A. and Solomatin A. V. The long-term earthquake prediction for the Kuril-Kamchatka island arc for the April 2016 through March 2021 period, its modification and application; the Kuril-Kamchatka seismicity before and after the May 24, 2013, M 8.3 deep-focus earthquake in the Sea of Okhotsk // Journal of Volcanology and Seismology. — 2017. — Vol. 11, no. 3. — P. 173–186. — https://doi.org/10.1134/S0742046317030022

Fedotov S. A. and Solomatin A. V. Long-Term Earthquake Prediction (LTEP) for the Kuril-Kamchatka island arc, June 2019 to May 2024; Properties of Preceding Seismicity from January 2017 to May 2019. The Development and Practical Application of the LTEP Method // Journal of Volcanology and Seismology. — 2019. — Vol. 13, no. 6. — P. 349–362. — https://doi.org/10.1134/S0742046319060022

Fedotov S. A., Solomatin A. V. and Chernyshev S. D. Long-term Earthquake Forecast for the Kuril-Kamchatka Arc for 2004-2008 and a Retrospective Forecast of the M = 8.1 September 25, 2003, Hokkaido Earthquake // Vulcanologiya i Sejsmologiya. — 2004. — No. 5. — P. 3–32. — (In Russian).

Fedotov S. A., Solomatin A. V. and Chernyshev S. D. A Long-term earthquake forecast for the Kuril-Kamchatka Island arc for the period 2006-2011 and a successful forecast of the MS = 8.2 middle Kuril earthquake of November 15, 2006 // Journal of Volcanology and Seismology. — 2007. — Vol. 1, no. 3. — P. 143–163. — https://doi.org/10.1134/s0742046307030013

Fedotov S. A., Solomatin A. V. and Chernyshev S. D. Aftershocks and the rupture zone of the Ms = 8.2, November 15, 2006 Middle Kuril Is. Earthquake and a long-term earthquake forecast for the Kuril-Kamchatka arc for the period from April 2008 to March 2013 // Journal of Volcanology and Seismology. — 2008. — Vol. 2, no. 6. — P. 375–394. — https://doi.org/10.1134/s0742046308060018

Fedotov S. A., Solomatin A. V. and Chernyshev S. D. A long-term earthquake forecast for the Kuril-Kamchatka arc for the period from September 2010 to August 2015 and the reliability of previous forecasts, as well as their applications // Journal of Volcanology and Seismology. — 2011. — Vol. 5, no. 2. — P. 75–99. — https://doi.org/10.1134/S0742046311020023

Fedotov S. A., Solomatin A. V. and Chernyshev S. D. A long-term earthquake forecast for the Kuril-Kamchatka arc for the period from September 2011 to August 2016. The likely location, time, and evolution of the next great earthquake with M ≥ 7.7 in Kamchatka // Journal of Volcanology and Seismology. — 2012. — Vol. 6, no. 2. — P. 65–88. — https://doi.org/10.1134/S0742046312020029

Gelfand I. M., Guberman Sh. A., Keilis-Borok V. I., et al. Conditions for the occurrence of strong earthquakes (California and some other regions) // Seismicity and Earth Modeling (Computational Seismology; Vol. 9). — Moscow : Nauka, 1976. — P. 3–91. — (In Russian).

Gordeev E. I., Fedotov S. A. and Chebrov V. N. Detailed seismological investigations in Kamchatka during the 1961-2011 period: Main results // Journal of Volcanology and Seismology. — 2013. — Vol. 7, no. 1. — P. 1–15. — https://doi.org/10.1134/S0742046313010041

Gvishiani A., Dobrovolsky M., Agayan S., et al. Fuzzy-based clustering of epicenters and strong earthquake-prone areas // Environmental Engineering and Management Journal. — 2013a. — Vol. 12, no. 1. — P. 1–10. — https://doi.org/10.30638/eemj.2013.001

Gvishiani A. D., Agayan S. M., Dobrovolsky M. N., et al. Objective epicenter classification and recognition of areas of large earthquakes possible occurrence in California // Geoinformatika. — 2013b. — No. 2. — P. 44–57. — (In Russian).

Gvishiani A. D., Dzeboev B. A. and Agayan S. M. FCaZm intelligent recognition system for locating areas prone to strong earthquakes in the Andean and Caucasian mountain belts // Izvestiya, Physics of the Solid Earth. — 2016. — Vol. 52, no. 4. — P. 461–491. — https://doi.org/10.1134/s1069351316040017

Gvishiani A. D. and Soloviev A. A. Study of areas prone to earthquakes with magnitude M ≥ 7.75 on the Pacific coast of South America // Doklady akademii nauk SSSR. — 1981. — Vol. 256, no. 5. — P. 1089–1091. — (In Russian).

Gvishiani A. D., Soloviev A. A. and Dzeboev B. A. Problem of Recognition of Strong-Earthquake-Prone Areas: a State-of-the-Art Review // Izvestiya, Physics of the Solid Earth. — 2020. — Vol. 56, no. 1. — P. 1–23. — https://doi.org/10.1134/s1069351320010048

Gvishiani A. D., Zelevinskii A. V., Keilis-Borok V. I., et al. Study of the areas of the violent earthquake occurrences in the Pacific Ocean belt with the help of recognition algorithms // Izvestiya AN SSSR. Fizika Zemli. — 1978. — No. 9. — P. 31–42. — (In Russian).

Gvishiani A. D., Zelevinskii A. V., Keilis-Borok V. I., et al. Recognition of locations of the strongest earthquakes in the Pacific belt (M > 8.2) // Methods and algorithms for interpreting seismological data (Computational Seismology; Vol. 13). — Moscow : Nauka, 1980. — P. 30–44. — (In Russian).

Gvishiani A. D., Zhidkov M. P. and Solov'yev A. A. Transfer of the High Seismicity Criteria of the Andes Mountainous Zones to Kamchatka // Izvestiya of the Academy of Sciences of the USSR. Physics of the Solid Earth. — 1984. — Vol. 20, no. 1. — P. 13–24.

Gvishiani A. D., Zhidkov M. P. and Soloviev A. A. Earthquake-prone areas recognition. X. Areas of earthquakes with magnitude M ≥ 7.75 on the Pacific coast of South America // Mathematical models of the Earth's structure and earthquake prediction (Computational Seismology; Vol. 14). — Moscow : Nauka, 1982. — P. 56–67. — (In Russian).

House L. S., Sykes L. R., Davies J. N., et al. Identification of a Possible Seismic Gap Near Unalaska Island, Eastern Aleutians, Alaska // Earthquake Prediction: An International Review / ed. by D. W. Simpson and P. G. Richards. — American Geophysical Union, 1981. — P. 81–92. — https://doi.org/10.1029/me004p0081

International Seismological Centre. ISC-GEM Earthquake Catalogue. — 2026. — https://doi.org/10.31905/d808b825

Jarrard R. D. Relations among subduction parameters // Reviews of Geophysics. — 1986. — Vol. 24, no. 2. — P. 217–284. — https://doi.org/10.1029/rg024i002p00217

Johnson J. M. and Satake K. Asperity Distribution of the 1952 Great Kamchatka Earthquake and its Relation to Future Earthquake Potential in Kamchatka // Pure and Applied Geophysics. — 1999. — Vol. 154, no. 3/4. — P. 541–553. — https://doi.org/10.1007/s000240050243

Johnson J. M., Tanioka Y., Ruff L. J., et al. The 1957 great Aleutian earthquake // Pure and Applied Geophysics. — 1994. — Vol. 142, no. 1. — P. 3–28. — https://doi.org/10.1007/bf00875966

Kagan Y. Y. and Jackson D. D. Seismic Gap Hypothesis: Ten years after // Journal of Geophysical Research: Solid Earth. — 1991. — Vol. 96, B13. — P. 21419–21431. — https://doi.org/10.1029/91JB02210

Kanamori H. The Alaska Earthquake of 1964: Radiation of long-period surface waves and source mechanism // Journal of Geophysical Research. — 1970. — Vol. 75, no. 26. — P. 5029–5040. — https://doi.org/10.1029/jb075i026p05029

Kanamori H. The energy release in great earthquakes // Journal of Geophysical Research. — 1977. — Vol. 82, no. 20. — P. 2981–2987. — https://doi.org/10.1029/JB082i020p02981

Kanamori H., Jennings P. C., Singh S. K., et al. Estimation of strong ground motions in Mexico City expected for large earthquakes in the Guerrero seismic gap // Bulletin of the Seismological Society of America. — 1993. — Vol. 83, no. 3. — P. 811–829. — https://doi.org/10.1785/BSSA0830030811

Kelleher J. A. Space-time seismicity of the Alaska-Aleutian Seismic Zone // Journal of Geophysical Research. — 1970. — Vol. 75, no. 29. — P. 5745–5756. — https://doi.org/10.1029/jb075i029p05745
Kelleher J. A. Rupture zones of large South American earthquakes and some predictions // Journal of Geophysical Research. — 1972. — Vol. 77, no. 11. — P. 2087–2103. — https://doi.org/10.1029/JB077i011p02087
Khan S. A. and Gudmundsson Ó. GPS analyses of the Sumatra-Andaman earthquake // Eos, Transactions American Geophysical Union. — 2005. — Vol. 86, no. 9. — P. 89–94. — https://doi.org/10.1029/2005eo090001
Konca A. O., Hjorleifsdottir V., Song T.-R. A., et al. Rupture Kinematics of the 2005 Mw 8.6 Nias-Simeulue Earthquake from the Joint Inversion of Seismic and Geodetic Data // Bulletin of the Seismological Society of America. — 2007. — Vol. 97, 1A. — S307–S322. — https://doi.org/10.1785/0120050632
Konovalov A. V., Stepnova Y. A. and Khanchuk A. I. Megathrust Earthquake off the Eastern Coast of Kamchatka on July 30, 2025 // Doklady Earth Sciences. — 2026. — Vol. 526, no. 2. — https://doi.org/10.1134/S1028334X25609137
Lallemand S., Heuret A. and Boutelier D. On the relationships between slab dip, back-arc stress, upper plate absolute motion, and crustal nature in subduction zones // Geochemistry, Geophysics, Geosystems. — 2005. — Vol. 6, no. 9. — Q09006. — https://doi.org/10.1029/2005gc000917
Lay T., Kanamori H., Ammon C. J., et al. The Great Sumatra-Andaman Earthquake of 26 December 2004 // Science. — 2005. — Vol. 308, no. 5725. — P. 1127–1133. — https://doi.org/10.1126/science.1112250
Lobkovsky L. I., Kerchman V. I., Baranov B. V., et al. Analysis of seismotectonic processes in subduction zones from the standpoint of a keyboard model of great earthquakes // Tectonophysics. — 1991. — Vol. 199, no. 2–4. — P. 211–236. — https://doi.org/10.1016/0040-1951(91)90173-p
Lobkovsky L. I., Shebalin P. N., Garagash I. A., et al. Possible Explanation for the Large Difference in Recurrence Periods of Megathrust Earthquakes in Kamchatka on July 29, 2025 and in Japan on March 11, 2011 // Doklady Earth Sciences. — 2026. — Vol. 528, no. 1. — P. 9. — https://doi.org/10.1134/s1028334x25610454
McCann W. R., Nishenko S. P., Sykes L. R., et al. Seismic gaps and plate tectonics: Seismic potential for major boundaries // Pure and Applied Geophysics. — 1979. — Vol. 117, no. 6. — P. 1082–1147. — https://doi.org/10.1007/bf00876211
Mikhailov V. O., Konvisar A. M., Smirnov V. B., et al. The Rupture Surface Model of the July 29, 2025 Mw 8.8 Kamchatka Earthquake Based on Satellite Geodesy and Interferometry Data // Doklady Earth Sciences. — 2025a. — Vol. 525, no. 2. — https://doi.org/10.1134/s1028334x25608752
Mikhailov V. O., Smirnov V. B., Timoshkina E. P., et al. Geodynamic Manifestations of Seismic Process in the Region of the November 15, 2006 and January 13, 2007 Simushir Earthquakes // Izvestiya, Physics of the Solid Earth. — 2025b. — Vol. 61, no. 4. — P. 586–598. — https://doi.org/10.1134/S1069351325700533
Mogi K. Some features of recent seismic activity in and near Japan (1) // Bulletin of the Earthquake Research Institute. — 1968. — Vol. 46. — P. 1225–1236.
Mogi K. Some features of recent seismic activity in and near Japan (2), activity before and after great earthquakes // Bulletin of the Earthquake Research Institute. — 1969. — Vol. 47. — P. 395–417.
Moreno M., Melnick D., Rosenau M., et al. Toward understanding tectonic control on the Mw 8.8 2010 Maule Chile earthquake // Earth and Planetary Science Letters. — 2012. — Vol. 321/322. — P. 152–165. — https://doi.org/10.1016/j.epsl.2012.01.006
Mori N., Takahashi T., Yasuda T., et al. Survey of 2011 Tohoku earthquake tsunami inundation and run-up // Geophysical Research Letters. — 2011. — Vol. 38, no. 7. — https://doi.org/10.1029/2011gl049210
Nikonov A. A. Kuril 1952 catastrophe, caused by a tsunami // Izvestiya Rossiiskoi Akademii Nauk. Seriya Geograficheskaya. — 2006. — No. 2. — P. 48–58. — (In Russian).
Nishenko S. P. Circum-Pacific seismic potential: 1989-1999 // Pure and Applied Geophysics. — 1991. — Vol. 135, no. 2. — P. 169–259. — https://doi.org/10.1007/bf00880240
Ojeda J., Ruiz S., Campo F. del, et al. The 21 May 1960 Mw 8.1 Concepción Earthquake: A Deep Megathrust Foreshock That Started the 1960 Central-South Chilean Seismic Sequence // Seismological Research Letters. — 2020. — Vol. 91, no. 3. — P. 1617–1627. — https://doi.org/10.1785/0220190143
Ozawa S., Nishimura T., Suito H., et al. Coseismic and postseismic slip of the 2011 magnitude-9 Tohoku-Oki earthquake // Nature. — 2011. — Vol. 475, no. 7356. — P. 373–376. — https://doi.org/10.1038/nature10227
Perez O. J. and Jacob K. H. Tectonic model and seismic potential of the eastern Gulf of Alaska and Yakataga Seismic Gap // Journal of Geophysical Research: Solid Earth. — 1980. — Vol. 85, B12. — P. 7132–7150. — https://doi.org/10.1029/jb085ib12p07132
Plata-Martinez R., Ide S., Shinohara M., et al. Shallow slow earthquakes to decipher future catastrophic earthquakes in the Guerrero seismic gap // Nature Communications. — 2021. — Vol. 12, no. 1. — P. 3976. — https://doi.org/10.1038/s41467-021-24210-9

Reisner G. I. and Rogozhin E. A. Seismotectonics and geodynamics of transition zones: The Kuril region // Vulcanologiya i Sejsmologiya. — 2003. — No. 1. — P. 42–53. — (In Russian).
Rong Y., Jackson D. D. and Kagan Y. Y. Seismic gaps and earthquakes // Journal of Geophysical Research: Solid Earth. — 2003. — Vol. 108, B10. — P. 2471. — https://doi.org/10.1029/2002jb002334
Schellart W. P., Jessell M. W. and Lister G. S. Asymmetric deformation in the backarc region of the Kuril arc, northwest Pacific: New insights from analogue modeling // Tectonics. — 2003. — Vol. 22, no. 5. — P. 1047–1064. — https://doi.org/10.1029/2002tc001473
Simons M., Minson S. E., Sladen A., et al. The 2011 Magnitude 9.0 Tohoku-Oki Earthquake: Mosaicking the Megathrust from Seconds to Centuries // Science. — 2011. — Vol. 332, no. 6036. — P. 1421–1425. — https://doi.org/10.1126/science.1206731
Solomatin A. V. Long-term earthquake prediction for the Kuril-Kamchatka arc for XII 2020 - XI 2025; medium-term seismic hazard assessment in the area of southern Kamchatka - northern Kuril Islands // Volcanism and related processes: Proceedings of the XXIV annual scientific conference dedicated to the Volcanologist Day. — Petropavlovsk-Kamchatsky : IViS FEB RAS, 2021. — P. 105–108. — (In Russian).
Solomatin A. V. Long-term seismic forecast for the Kuril-Kamchatka Arc for III.2022-II.2027; analysis of the results of the medium and short-term forecast for the Paramushir Island area, given for autumn 2021 // Volcanism and related processes: Proceedings of the XXV annual scientific conference dedicated to the Volcanologist Day. — Petropavlovsk-Kamchatsky : IViS FEB RAS, 2022. — P. 107–110. — (In Russian).
Solomatin A. V. Long-term earthquake prediction for the Kuril-Kamchatka arc for I 2024 - XII 2028; the concept of statistical confidence in seismic monitoring of geodynamic processes // Volcanism and related processes: Proceedings of the XXVII annual scientific conference dedicated to the Volcanologist Day. — Petropavlovsk-Kamchatsky, 2024. — P. 191–194. — in Russian.
Solomatin A. V. and Soldatov P. D. Long-term seismic forecast for II 2023-I 2027. Concept of methodology for monitoring of geofluidodynamic processes in the region based on plane-oriented clusters // Volcanism and related processes: Proceedings of the XXVI annual scientific conference dedicated to the Volcanologist Day. — Petropavlovsk-Kamchatsky : IViS FEB RAS, 2023. — P. 104–107. — (In Russian).
Storchak D. A., Di Giacomo D., Bondar I., et al. Public Release of the ISC-GEM Global Instrumental Earthquake Catalogue (1900-2009) // Seismological Research Letters. — 2013. — Vol. 84, no. 5. — P. 810–815. — https://doi.org/10.1785/0220130034
Storchak D. A., Di Giacomo D., Engdahl E. R., et al. The ISC-GEM Global Instrumental Earthquake Catalogue (1900-2009): Introduction // Physics of the Earth and Planetary Interiors. — 2015. — Vol. 239. — P. 48–63. — https://doi.org/10.1016/j.pepi.2014.06.009
Sykes L. R. Aftershock zones of great earthquakes, seismicity gaps, and earthquake prediction for Alaska and the Aleutians // Journal of Geophysical Research. — 1971. — Vol. 76, no. 32. — P. 8021–8041. — https://doi.org/10.1029/JB076i032p08021
Tarakanov R. Z., Levyi N. V. and Kim Ch. U. Seismicity of the Kuril region // Seismic Zoning of the Kuril Islands, Primorye and Priamurye. — Vladivostok : Far Eastern Scientific Center of the USSR Academy of Sciences, 1977. — P. 27–35. — (In Russian).
USGS. M 8.8 - 2025 Kamchatka Peninsula, Russia Earthquake. — 2025. — URL: https://earthquake.usgs.gov/earthquakes/eventpage/pt25210002/executive.
Vigny C., Socquet A., Peyrat S., et al. The 2010 Mw 8.8 Maule megathrust earthquake of Central Chile, monitored by GPS // Science. — 2011. — Vol. 332, no. 6036. — P. 1417–1421. — https://doi.org/10.1126/science.1204132
Vorobieva I. A., Gvishiani A. D., Dzeboev B. A., et al. Nearest Neighbor Method for Discriminating Aftershocks and Duplicates When Merging Earthquake Catalogs // Frontiers in Earth Science. — 2022. — Vol. 10. — P. 820277. — https://doi.org/10.3389/feart.2022.820277
Wilson J. T. A possible origin of the Hawaiian Islands // Canadian Journal of Physics. — 1963. — Vol. 41, no. 6. — P. 863–870. — https://doi.org/10.1139/p63-094
Yuan X., Li X., Wölbern I., et al. Tracing the Hawaiian Mantle Plume by Converted Seismic Waves // Mantle Plumes / ed. by J. R. R. Ritter and U. R. Christensen. — Berlin, Heidelberg : Springer Berlin Heidelberg, 2007. — P. 49–69. — https://doi.org/10.1007/978-3-540-68046-8_2